Biogeosciences, 21, 3883–3902, 2024
https://doi.org/10.5194/bg-21-3883-2024

Biogeosciences Open Access EGU

Global and regional hydrological impacts of global forest expansion

James A. King[1], James Weber[1,a], Peter Lawrence[2], Stephanie Roe[3], Abigail L. S. Swann[4], and Maria Val Martin[1]

[1]Leverhulme Centre for Climate Change Mitigation, School of Biosciences, University of Sheffield, Sheffield, UK
[2]Climate and Global Dynamics Laboratory, National Center for Atmospheric Research, Boulder, CO, USA
[3]World Wildlife Fund, Washington, DC, USA
[4]Department of Atmospheric Science and Department of Biology, University of Washington, Seattle, WA, USA
[a]now at: Department of Meteorology, University of Reading, Reading, UK

Correspondence: James A. King (james.king@sheffield.ac.uk)

Received: 11 March 2024 – Discussion started: 21 March 2024
Revised: 5 June 2024 – Accepted: 5 July 2024 – Published: 3 September 2024

Abstract. Large-scale reforestation, afforestation, and forest restoration schemes have gained global support as climate change mitigation strategies due to their significant carbon dioxide removal (CDR) potential. However, there has been limited research into the unintended consequences of forestation from a biophysical perspective. In the Community Earth System Model version 2 (CESM2), we apply a global forestation scenario, within a Paris Agreement-compatible warming scenario, to investigate the land surface and hydroclimate response. Compared to a control scenario where land use is fixed to present-day levels, the forestation scenario is up to 2 °C cooler at low latitudes by 2100, driven by a 10 % increase in evaporative cooling in forested areas. However, afforested areas where grassland or shrubland are replaced lead to a doubling of plant water demand in some tropical regions, causing significant decreases in soil moisture (∼ 5 % globally, 5 %–10 % regionally) and water availability (∼ 10 % globally, 10 %–15 % regionally) in regions with increased forest cover. While there are some increases in low cloud and seasonal precipitation over the expanded tropical forests, with enhanced negative cloud radiative forcing, the impacts on large-scale precipitation and atmospheric circulation are limited. This contrasts with the precipitation response to simulated large-scale deforestation found in previous studies. The forestation scenario demonstrates local cooling benefits without major disruption to global hydrodynamics beyond those already projected to result from climate change, in addition to the cooling associated with CDR. However, the water demands of extensive forestation, especially afforestation, have implications for its viability, given the uncertainty in future precipitation changes.

1 Introduction

The need to achieve net zero carbon emissions in order to reach the Paris Agreement climate targets demonstrates the importance of drastic emissions reductions as well as effective carbon dioxide (CO_2) removal (CDR) (Fankhauser et al., 2021). Enhancing the capacity of the terrestrial biosphere to absorb and store CO_2, including through afforestation (planting trees on previously unforested land), reforestation (planting trees on previously forested land), and forest restoration (repairing degraded forests), has emerged as an important strategy for climate change mitigation (Girardin et al., 2021; IPCC, 2022; Roe et al., 2021). Indeed, the full realisation of countries' Paris Agreement commitments would result in forests absorbing $1.1 \pm 0.5\,\mathrm{Gt\,CO_2e\,yr^{-1}}$ by 2030, representing one-quarter of planned emissions reductions (Grassi et al., 2017; Smith et al., 2023). In addition to national climate commitments, countries and private sector actors have made global restoration commitments, including the UN Decade on Ecosystem Restoration and the Bonn Challenge, in which 74 countries initially agreed to restore 350 Mha of degraded land by 2030. This has since increased to 115 countries and up to 1000 Mha of land restoration by 2040 (Sewell et al., 2020). A wide range of private sector and non-governmental land and forest restoration commitments,

as well as tree planting initiatives, have also been launched in recent years (Martin et al., 2021; Seddon et al., 2021).

CDR potential, as it relates to climate change mitigation potential, is generally estimated by calculating the amount of carbon sequestered from the atmosphere by a given intervention compared to a counterfactual scenario without the intervention. Several recent studies have attempted to quantify the CDR potential of global-scale reforestation, afforestation, and forest restoration, with variable estimates resulting from different methodological approaches (e.g. Griscom et al., 2017; Roe et al., 2019; Seddon et al., 2021). For example, Bastin et al. (2019) suggested that an additional 900 Mha of tree cover could potentially exist with an additional storage capacity of 205 Pg C, although the magnitude of this CDR potential was argued to be several times overestimated (Friedlingstein et al., 2019; Lewis et al., 2019a). Lewis et al. (2019b) gave an estimate of 1200 Mha of suitable land area for restoring natural forest ecosystems while estimating a maximum storage capacity of 42 Pg C by 2100 for the initially committed Bonn Challenge land area if it is entirely given over to forest restoration (144 Pg C for the maximum possible area). Griscom et al. (2017) found that estimates of potential reforestation area ranged from 345–1779 Mha and defined their own 678 Mha "area of opportunity" for the regrowth of natural forests. Cook-Patton et al. (2020) used this area to derive a maximum biosphere CDR potential of 2.43 Pg C yr^{-1} by 2050.

Beyond carbon sequestration, it is also important to estimate the broader climate impacts of large-scale forest expansion (Seddon et al., 2020). Forests influence climate in complex ways and at multiple spatial scales (Bonan, 2008, 2016), which can broadly be categorised into biogeophysical and biogeochemical. Biogeophysical impacts result from changes to the surface energy balance. These include the effect of the reduced albedo (i.e. the ratio of reflected to incident radiation) of trees when compared to other land cover types, such as cropland or grassland (Kirschbaum et al., 2011; Windisch et al., 2021). The albedo effect is particularly pronounced for expansion of forests over previously snow-covered tundra landscapes (De Wit et al., 2014; Bonan et al., 1992), which reduces the climate mitigation potential of forest expansion in high-latitude regions such as northern Canada (Drever et al., 2021). Other less well understood biogeophysical impacts include changes to soil moisture and evapotranspiration (Nosetto et al., 2005), which can affect both temperature (through changes to surface energy balance; Barnes et al., 2024) and rainfall (through changes to cloud cover; Duveiller et al., 2021). Locally, this can have both positive and negative impacts on extreme weather events (Abiodun et al., 2013). Observational studies have found links between forest cover and convective clouds over tropical rainforests (Bekenshtein et al., 2023), where evapotranspiration is a key driver of rainfall (Crowhurst et al., 2021), as well as over temperate forests where frontally generated clouds are more common than deep convective clouds (Duveiller et al., 2021; Wang et al., 2009). Hua et al. (2023) showed that tropical deforestation can reduce local cloud cover, and Xu et al. (2022) suggested that the background sensible heat flux determines the sign of the response to forest cover change. In tropical regions, the effects of large-scale forestation or deforestation in low latitudes are typically dominated by the impacts on cloud processes through increasing low-level humidity and latent heating along with cloud condensation nuclei (CCN) increases (Bekenshtein et al., 2023). In the tropical troposphere, deep convection is driven by strong latent heating as a result of high humidity near the surface. Much of this convection is driven by evapotranspiration from tropical rainforests, though the extent to which this is true varies depending on the domain in question (C. Smith et al., 2023).

At continental and hemispheric scales, increased moisture availability can drive changes in latent heating (i.e. energy released due to the condensation of water vapour) that affect remote atmospheric dynamics (Laguë et al., 2021), including the general circulation of the atmosphere (Portmann et al., 2022). Increased soil water demand from the land use change from grassland or cropland to forest has implications for water supply to both forests themselves and nearby communities (Hoek van Dijke et al., 2022). Biogeochemical impacts of forest expansion beyond carbon sequestration derive from increased emissions of biogenic volatile organic compounds (BVOCs) such as isoprene (Bonan, 2008; Šimpraga et al., 2019). BVOCs undergo complex chemical reactions in the troposphere, including oxidation to form secondary organic aerosols (SOAs) (Sporre et al., 2019; Zhang et al., 2023); they also affect air quality with implications for human health (Heald and Spracklen, 2015; Val Martin et al., 2015) and food security (Tai et al., 2014). The chemical processes which BVOCs undergo in the atmosphere affect tropospheric concentrations of the greenhouse gases CH_4 and O_3, organic aerosols, and cloud properties, with radiative impacts which, when combined with albedo, may offset up to one-third of the climate mitigation benefits from forest-based CDR, depending on the level of future warming (Weber et al., 2024; Zhang et al., 2023). In this analysis we focus on the biogeophysical and hydrological impacts on the land surface and clouds while noting that BVOC chemistry and hydrology are not separable because of the impact of the former on radiative forcing, cloud nucleation, and other important processes.

While there is a substantial body of literature on the interactions between forests and climate (Bonan, 2016), which increasingly incorporates recent advances in satellite-based remote sensing and Earth system modelling, there has been less attention given to evaluating the consequences of forest-based CDR strategies beyond attempts to quantify their carbon sequestration potential, despite the prominence of these strategies in the policy sphere. Recent advances have been made from observations of forest cover change affecting low-level clouds (Duveiller et al., 2021) and from the application

of idealised forest cover scenarios to identify changes in atmospheric circulation (Portmann et al., 2022). There has also been much recent attention given to the climate impacts of deforestation (Alkama and Cescatti, 2016; Bala et al., 2007; Boysen et al., 2020; Lawrence et al., 2022; Lee et al., 2023; Bekenshtein et al., 2023; C. Smith et al., 2023; Swann et al., 2015), but it is not clear whether the processes by which deforestation affects climate are reversible in the case of deliberate increases in forest cover. There is therefore a need to evaluate and estimate the broader climate impacts from plausible forestation proposals in the context of climate change mitigation (Fuhrman et al., 2020; Orlov et al., 2023; Zickfeld et al., 2023), in particular reflecting the necessity that such mitigation is just (Robinson and Shine, 2018; Fleischman et al., 2020) and avoids placing a mitigation burden on the Global South in response to emissions from the Global North (Bond et al., 2019; Parr et al., 2024). In this study, we use an Earth system modelling framework to investigate the impacts of large-scale forest expansion on the water cycle. We first assess how such a global-scale scenario influences key processes at the land surface; secondly, we examine the potentially meaningful effects on cloud cover, precipitation, and atmospheric circulation.

2 Methods

Investigating global forest–climate interactions necessitates the use of a fully coupled Earth system model (ESM) which simulates feedbacks between the terrestrial biosphere, atmosphere, and oceans. We use version 2.1.3 of the Community Earth System Model (CESM2; Danabasoglu et al., 2020) at $0.9° \times 1.25°$ horizontal resolution. The atmospheric component is the Community Atmosphere Model version 6 with the MOZART troposphere–stratosphere (TS1) chemistry mechanism (CAM6-Chem; Emmons et al., 2020) and the four-mode version of the Modal Aerosol Model (MAM4; Liu et al., 2016). The model has a 32-layer atmosphere extending to ~ 3 hPa, with prescribed stratospheric aerosols above the model top. The land model is the Community Land Model version 5 (CLM5; Lawrence et al., 2019) with prognostic vegetation and fully active biogeochemistry, which incorporates the Model of Emissions and Gases from Nature version 2.1 (MEGAN2.1; Guenther et al., 2012). The ocean model used is the Parallel Ocean Program version 2 (POP2; Danabasoglu et al., 2012). The model configuration employed is similar to that used in the CESM2 contribution to ScenarioMIP but with the addition of a prognostic atmospheric chemistry scheme.

To evaluate the impacts of global-scale forestation, we performed three sets of model experiments which differed only in the prescribed land use and land cover change (LULCC). All model experiments were forced using prescribed well-mixed greenhouse gases (WMGHGs, such as CO_2, CH_4, and N_2O) as fixed lower boundary conditions following the SSP1-2.6 scenario. This scenario is consistent with the Paris Agreement targets as it results in a global mean surface temperature increase by 2100 relative to pre-industrial conditions of ~ 1.7 °C (Gidden et al., 2019). We use this emissions scenario because we assume that a world in which large-scale forest expansion is implemented is a world in which climate change mitigation is prioritised and where Paris-compatible measures on emissions reduction are also implemented. We also prescribe SSP1-2.6 non-GHG anthropogenic emissions (e.g. from biomass burning, aircraft, and shipping). Anthropogenic emissions are derived from the Community Emissions Data System (CEDS; Hoesly et al., 2018) and biomass burning from Input4MIPs (Gidden et al., 2019). Biogenic emissions are actively simulated by MEGAN. We do not consider the role of fire in this study, nor other vegetation disturbances such as surface ozone damage, herbivory, and diseases, as our aim is to isolate the hydrological impacts directly caused by forest expansion, rather than second-order feedbacks that could obscure the direct signals; herbivory and disease are not simulated explicitly by CLM5, while frost damage and heat stress are included implicitly in the model (Lawrence et al., 2019).

The control model experiment (SSP1-2.6 without LULCC, or "No LULCC") follows SSP1-2.6 GHGs and anthropogenic emissions, but LULC data are fixed at 2015 levels based on the incorporation into CLM5 of historical data from the Land-Use Harmonization transient dataset version 2 (LUH2; Lawrence et al., 2016). In this setup, the biosphere can respond to changes in climate and CO_2 fertilisation through photosynthesis and leaf area index (LAI), for example, but the proportion of each grid cell covered by each land use type is fixed. The next set of model experiments (SSP1-2.6, or "Base") followed the SSP1-2.6 LULCC trajectory from ScenarioMIP. This represents a well-established reference point for a Paris-compatible future and serves as a moderate reforestation scenario in which tree cover increases globally by 10 % by 2100 compared to 2015, an increase of ~ 300 Mha, but there is also some deforestation and expansion of agricultural land at a regional level.

The model experiment with large-scale forestation (SSP1-2.6 Max Forest, or "Max Forest") used a scenario developed by Roe (2021) within CLM5, also used in Weber et al. (2024), to evaluate the climate change mitigation potential of reforestation (of rangeland, secondary forest, and secondary non-forest in forest biomes), afforestation (of rangeland, secondary forest, and secondary non-forest in non-forest biomes where tree cover is greater than 10 %), and forest enhancement (of forests where tree cover density is less than its potential). Global forest cover expands by 26 % by 2100 compared to 2015, an increase of ~ 750 Mha, well within the range of previous estimates (Griscom et al., 2017). This scenario achieves an average rate of CDR under SSP1-2.6 GHG forcing of $5.1\,\mathrm{Gt\,CO_2\,yr^{-1}}$ by 2050 (Roe et al., 2021), which is within the ranges found in previous studies (Lawrence et al., 2018; Nabuurs et al., 2023). The total cumulative bio-

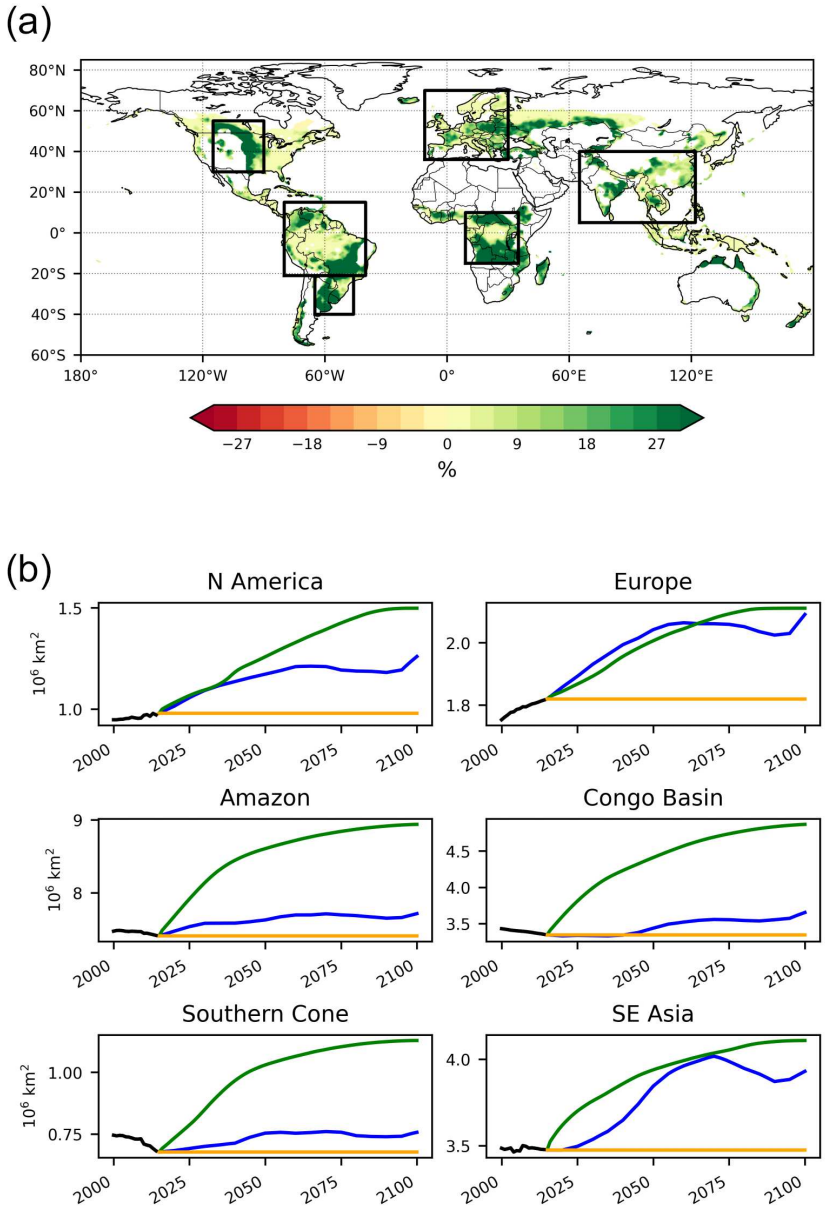

Figure 1. The Max Forest scenario in the context of the shared socioeconomic pathways (SSPs). **(a)** Percentage increase in forest cover, 2095 minus 2015, with boxes showing the different regional domains. **(b)** Regional changes in total forest area for Base (blue), Max Forest (green), and No LULCC (orange) model experiments. Historical data from LUH2 for 2000–2014 are shown in black.

sphere C sequestration in Max Forest by 2095 under SSP1-2.6 CO_2 is roughly 410 Gt C, which is in line with the estimated additional forest CDR potential of 221–472 Gt C (Mo et al., 2023). We define the "Max Forest" scenario using the maximum values of all three forest expansion strategies evaluated by Roe et al. (2021). The scenario operates by expanding areas of existing forest cover into suitable area as defined by a bioclimatic envelope approach (Whittaker, 1975). This avoids planting trees in areas where they would be unlikely to grow, such as arid environments; it also ensures a realistic distribution of plant functional types (PFTs) suitable for each biome. This approach has the additional benefit of limiting high-latitude tree growth in existing tundra environments while concentrating forest expansion at the margins of tropical rainforests (Fig. 1), aiming to minimise the enhanced local warming associated with albedo decrease in cold tundra while maximising the local evaporative cooling associated with tropical rainforests (Roe et al., 2021). The scenario also excludes forestation in International Union for Conservation of Nature (IUCN)-designated protected areas in an effort to limit potential negative impacts on existing biodiversity and ecosystem structure and function; there is substantial overlap

(42 %) between areas of forest restoration in this scenario and priority areas for biodiversity conservation and ecosystem service provision under the "Sharing the Planet" scenario (Kok et al., 2023). Food security concerns around forest expansion are addressed by fixing agricultural areas at 2015 levels and preventing forest from encroaching upon them. The Max Forest scenario thus presents a biophysical maximum for forest expansion in the 21st century which considers global priorities around biodiversity and food security as well as climate change. In addition, Max Forest is comparable to existing ambitious targets for land restoration, including the Bonn Challenge targets, as well as current global restoration commitments ("GRCs") – although the latter also include non-forest restoration (Sewell et al., 2020) (Fig. S1 in the Supplement). We select six main regional domains (North America, Europe, Amazon Basin, Congo Basin, South and East Asia, and the Southern Cone; Fig. 1a) as they represent areas with large tree cover, and we show results for the globe alongside the Congo and Amazon basins, as these tropical rainforest basins are global priorities for forest restoration. Detail on other domains is provided in the Supplement.

In order to account for the process of model internal variability arising from the use of a fully coupled land–ocean–atmosphere experimental setup, three ensemble members were run for each model experiment using varying initial conditions for 2015 taken from the endpoint of different historical runs of CESM2 from ScenarioMIP. This approach provided us with initial conditions which were "spun up" but also represented a reasonable sample of the uncertainty associated with simulating the present-day state of the Earth system. The analysis presented here refers to the ensemble means for each model experiment. Each ensemble member was run from 2015–2100 to control for internal climate variability, such as the El Niño–Southern Oscillation (ENSO). We take decadal mean values from 2015–2025 to represent "2020", 2045–2055 for "2050", and 2090–2100 for "2095" in the analysis.

3 Results

3.1 Changes to land surface processes

We first demonstrate that forest expansion can have direct climate mitigation benefits by reducing surface temperatures. Figure 2 shows the effect of forestation on near-surface temperatures. In the Max Forest scenario, near-surface air temperatures in forested areas are on a global average 0.48 °C cooler than the No LULCC and 0.38 °C cooler than Base by the end of the 21st century. Zonally averaged tropical near-surface air temperatures in the northern (southern) tropics are up to 0.55 °C (0.75 °C) cooler in Max Forest compared to No LULCC in 2095 (Fig. 2a). Figure 2 demonstrates that the Max Forest scenario effectively removes the global warming signal from the Congo Basin domain, as there is effectively no warming at 2050 or 2095 relative to 2015 and a small but significant cooling (~ 2 %) over the areas where forest cover increases most (Fig. 2b). The Max Forest scenario is also significantly cooler in the most forested parts of the Amazon Basin than both SSP1 Base and No LULCC at 2050 and 2095 (Fig. 2b). The Max Forest scenario is up to 2 °C cooler than in the No LULCC scenario at the margins of tropical rainforest basins, in particular central Africa, southern Brazil, Colombia and Venezuela, and northern Australia, which are key targets for forest expansion in the scenario. It is important to note that GHG concentrations were prescribed following SSP1-2.6 in our model experiments. Consequently, the cooling effect due to CDR is purely biophysical and not due to any change in the atmospheric concentration of CO_2. Figure 2a shows some near-surface warming in the central USA and the Russian–Kazakh border which is driven by local albedo decreases (Fig. S2). The North America domain is ~ 0.2 °C warmer at the end of the 21st century in Max Forest compared to No LULCC. However, this temperature difference is not statistically significant at the 95 % confidence level (Fig. 2a). Much of the Northern Hemisphere midlatitudes are cooler in the Base than in the Max Forest scenario, as the greatest temperature differences between the scenarios are located over the Canadian Arctic where neither scenario changes forest cover. This effect may be related to sea surface temperature (SST) biases in the Labrador Sea in CESM2 (Danabasoglu et al., 2020).

Beyond affecting temperatures on global and regional scales, large-scale forestation also affects key climate-relevant processes at the land surface. In our scenario, the biosphere response to CO_2 is an upper bound, as plants take up CO_2 from the atmosphere but do not deplete it. Between 2015 and 2095 in the Congo Basin, net primary productivity (NPP) in Max Forest increases by $2.1\,\mathrm{Pg\,C\,yr^{-1}}$ (33 %) compared to 2015 levels, while the No LULCC scenario exhibits an increase of only $\sim 0.5\,\mathrm{Pg\,C\,yr^{-1}}$ (Fig. S3). Increased photosynthetic activity by plants in this domain drives concurrent increases in evapotranspiration (Fig. 3). In the Congo Basin, this increases by $0.2\,\mathrm{mm\,d^{-1}}$ by 2100. This increased evapotranspiration in warm, humid environments drives evaporative cooling of the surface through latent heat release (Figs. 3 and 4), accounting for the reduction in surface warming seen in the tropics in Max Forest (Fig. 2).

Replacing areas of grassland or shrubland with forest can be expected to increase water demand, and consequently water stress (where demand approaches or exceeds supply) can increase if there are no corresponding increases in precipitation. This can be exacerbated under conditions of elevated CO_2 and moderate temperature increases, which can increase plant productivity if that increase in productivity outweighs water savings associated with increases in water use efficiency under elevated CO_2. We use the vegetation water potential (veg WP) as a metric for water stress in CLM5 (Kennedy et al., 2019). This quantity reflects both root and leaf hydraulics, and increasing (more negative) values reflect

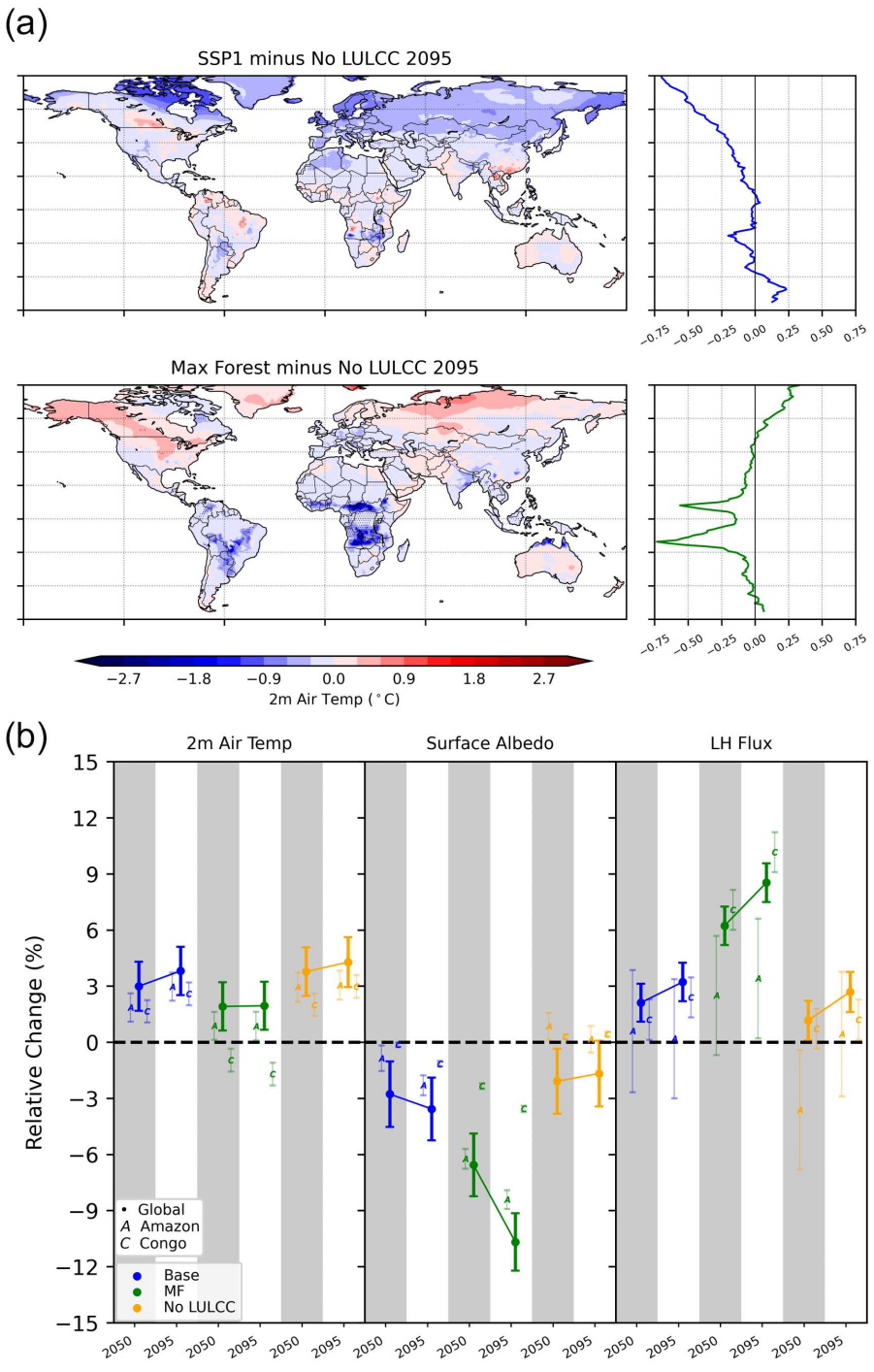

Figure 2. Air temperature at 2 m above the land surface. **(a)** Global changes at 2095 between Base (top) and Max Forest (bottom) and No LULCC. Stippling denotes statistical significance of differences assessed using a two-tailed Student T test at $\alpha = 0.05$; zonal means of the differences are shown on the right. **(b)** Area-weighted mean values for 2 m air temperature, surface albedo, and latent heat flux, for grid cells where the increase in tree cover between 2015 and 2095 > 25 %, expressed as percentage differences from the 2020 mean for No LULCC. For each model experiment the left point indicates the 2050 (2045–2055) mean and the right point the 2095 (2090–2100) mean. Circles indicate the global mean, "A" the Amazon Basin, and "C" the Congo Basin. Error bars denote the standard error of the decadal means expressed as percentage differences (U.S. Census Bureau, 1998). Colours are blue for SSP-2.6 Base, green for Max Forest, and orange for No LULCC.

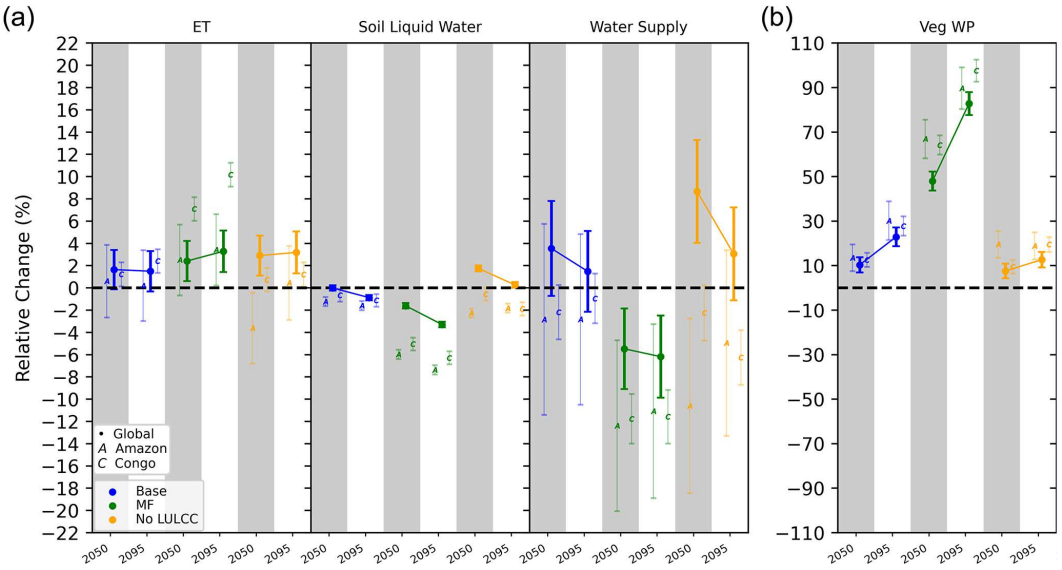

Figure 3. As Fig. 2b but for the annual sum of mean evapotranspiration (ET), vertically averaged soil liquid water content, water supply (runoff + river flow) **(a)**, and vegetation water potential **(b)**.

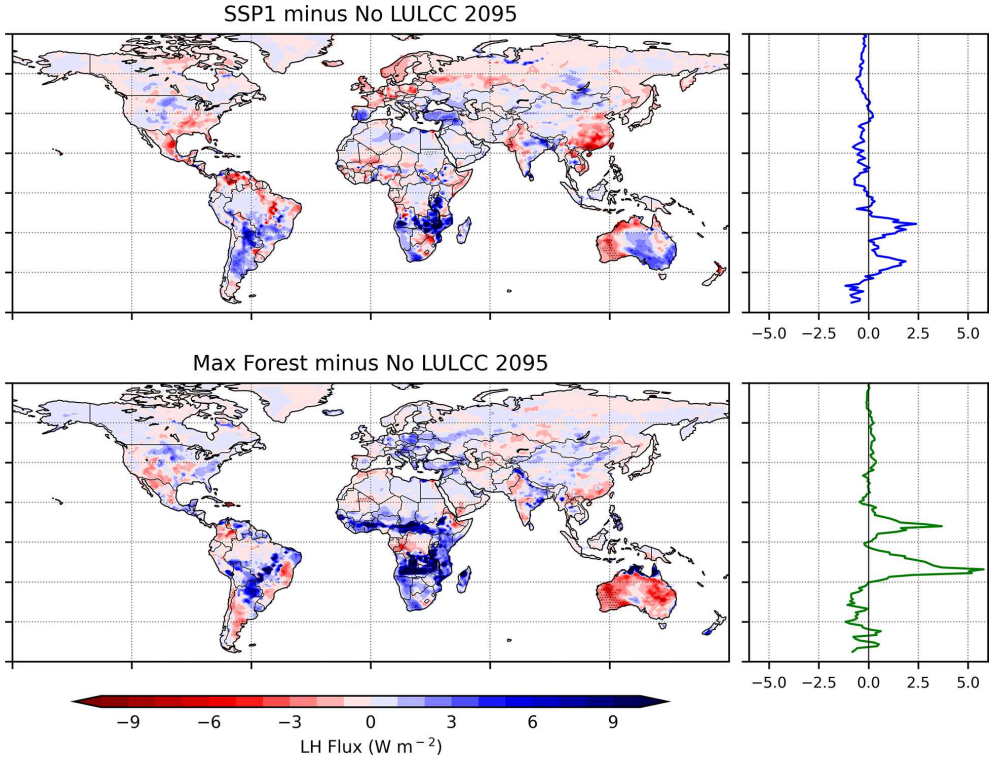

Figure 4. As Fig. 2a but showing the differences in surface latent heat flux between model experiments at the end of the 21st century.

increases in water demand from plants as plant size increases (e.g. from grasses to trees). Stronger veg WP increases are found in Max Forest than in the other scenarios. Globally, in Max Forest, veg WP increases by 47 % in 2050 and 82 % in 2095 relative to 2020 values. In contrast, the Base scenario has moderate increases of 10 % in 2050 and 22 % in 2095, while the No LULCC scenario exhibits an even lower increase, with 8 % in 2050 and 11 % in 2095 (Fig. 3). Regionally, changes in Max Forest vary from a ∼ 66 % increase in North America to a ∼ 100 % increase in tropical rainfor-

est areas by 2095. Our results further indicate significant decreases in soil liquid water content in the Max Forest scenario in all domains apart from Europe (Figs. 3 and S6) compared to the other scenarios, which reflects a situation where plant water demand as a result of extensive forest expansion may be exceeding soil water supply across the globe. This corresponds to a global-scale decrease in surface water supply (expressed as the sum of the surface runoff and river flow) of between 5 % and 10 % and between 10 % and 15 % in the Amazon and the Congo basins, respectively (Fig. 3).

3.2 Changes in cloud cover

We assess the effects of forestation in cloud cover and related processes such as the density of CCN in Figs. 5 and 6.

In our results, we find significant increases in low cloud fraction over Argentina in Base relative to No LULCC in 2095. In Max Forest, there are small but significant increases (~ 5 %) in low-level cloud fraction (below 700 hPa) over the Congo Basin, northern Australia, Uruguay, and Colombia and Venezuela in 2095 (Fig. 5a) with smaller yet significant increases of the same spatial pattern in 2050. All of these are areas with significant increases in tree cover in Max Forest. Significant differences in oceanic low cloud of both positive and negative signs are seen in both scenarios relative to No LULCC (Fig. 5a). However, given the moderate nature of our land use change scenarios, attributing these changes directly to forestation is challenging. While low cloud cover is important for the surface radiation balance, changes to deep convective clouds over the tropical rainforest basins can have important consequences for regional and global climate. We find statistically significant but small (~ 0.2 %) increases in tropical convective cloud fraction over Africa in Max Forest relative to No LULCC in 2095 (Fig. 5b), but the significant differences are restricted to below 900 hPa, implying a limited effect of the land use change scenario on deep convection.

In addition to the amount of cloud cover, which is affected by evapotranspiration, forestation can also influence cloud properties such as water content and the concentrations of cloud condensation nuclei (CCN). Trees provide a source of BVOCs as a by-product of a number of biological processes, and BVOC emissions are elevated during warmer conditions (Weber et al., 2022). BVOC chemistry can result in the growth and formation of secondary organic aerosols (SOAs), which act as CCN. This effect can clearly be seen in Fig. 6a, where CCN concentration at 0.1 % supersaturation is significantly greater (up to $+1000\,\mathrm{cm}^{-3}$) over areas of increased forest cover in Max Forest at 2095 compared to No LULCC. The signal is particularly strong in the tropics due to this temperature dependence but is also significant in the central USA, implying synergies between tree type and climate in this location that are less active elsewhere in the midlatitudes (Sindelarova et al., 2014) and may be related to the expansion of deciduous forest in the USA which is more emissive of isoprene (Guenther et al., 2012). A similar pattern is evident when the Base scenario is compared to No LULCC. Figure 6b shows the in-cloud liquid water path (LWP), a measure of the mass of water droplets in each model layer. There are statistically significant increases in LWP over land in tropical Africa and Australia in Max Forest compared to No LULCC, but the magnitude is small ($< 1\,\mathrm{g\,m}^{-3}$). Differences over the tropical Pacific in both SSP1 Base and Max Forest are likely a response to SST pattern changes, as also observed for cloud fraction (Fig. 5). We find similar results for CCN and LWP in 2050 but with a smaller signal, in line with the changes in low cloud fraction.

The total cloud forcing or cloud radiative effect (CRE) summarises the impact of clouds on the Earth's radiative balance and is affected by cloud fraction (i.e. cloud cover), cloud height, and cloud reflectivity (which is in turn affected by cloud water and CCN concentration). For a given scenario and time period, the CRE is calculated as the difference in net incoming top-of-atmosphere (TOA) radiation between a case in which clouds are included in the radiation scheme and a case where the interaction of clouds with radiation is ignored (a so-called "clear" diagnostic); in both cases a double call to the radiation scheme is used to remove the scattering due to aerosols (a so-called "clean" diagnostic) following Weber et al. (2024). A comparison of the CRE between two scenarios or time points (e.g. SSP1 Base at 2020 and 2050), termed "forcing" here, illustrates how changes to cloud cover and cloud properties have affected the Earth's energy budget. These effects can be decomposed into shortwave (SW) and longwave (LW) components.

Figure 7 shows that in the Base, Max Forest, and No LULCC scenarios, the total and SW cloud forcing is positive at 2050 and 2095 relative to 2020. While clouds have a net cooling effect on the Earth in each scenario and time period, this finding indicates that the changes to clouds in 2050 and 2095 mean this cooling effect is smaller than in 2020. However, this positive forcing is smaller in the Max Forest scenarios than in either Base or No LULCC, corresponding to Max Forest's smaller decrease in low cloud cover on a global scale.

Regionally, statistically significant forcings of ~ -2 to $-3\,\mathrm{W\,m}^{-2}$ are found over parts of the Congo Basin, SE Asia, the Southern Cone, and northern Australia (Fig. S8). This is also consistent with a shortwave cooling effect associated with increased low cloud cover in the tropics, due to increased reflection of incoming shortwave radiation, while changes to deep convective clouds are limited in our model experiments (Fig. 5b). There is also some cooling over land in Europe which is related to small increases in shortwave cooling (Fig. S8); however, the negative CRE change here is not statistically significant.

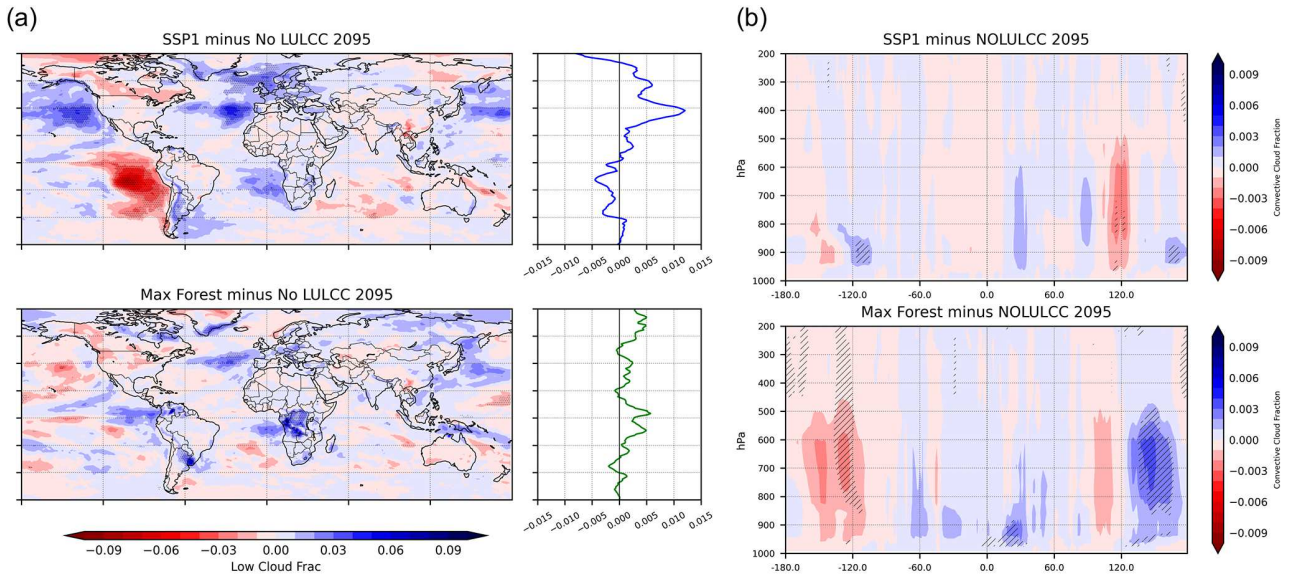

Figure 5. **(a)** Differences between model experiments at the end of the 21st century in cloud cover integrated vertically between 1200–700 hPa. **(b)** As in **(a)** but showing vertical cross-sections of convective cloud cover averaged across tropical latitudes. Hatching in **(b)** denotes statistical significance of differences assessed using a two-tailed Student T test at $\alpha = 0.05$.

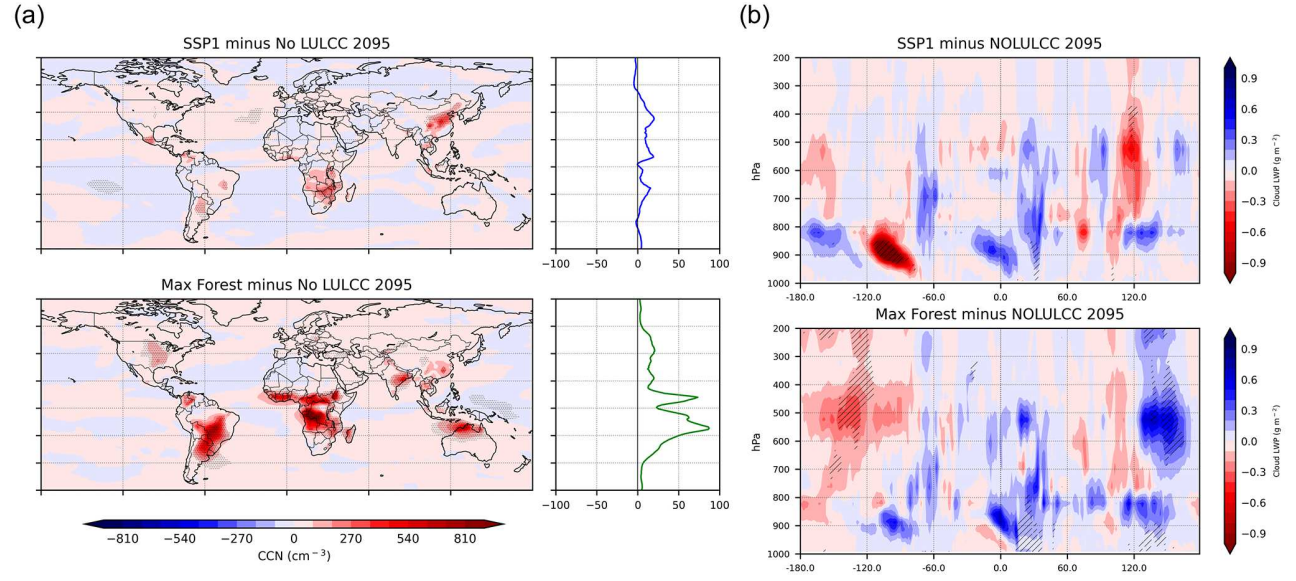

Figure 6. **(a)** The vertical sum of cloud condensation nuclei (CCN) at 0.1 % supersaturation and **(b)** the total in-cloud liquid water path (LWP). Note the reversed colour scale in **(b)**.

3.3 Effects on precipitation and atmospheric dynamics

Owing to the smaller increase in forest expansion in our scenario compared with other, more idealised studies, as well as the moderate climate change scenario selected, substantial impacts on global precipitation are expected to be limited (especially given the small changes to cloud cover shown in Fig. 5). However, regional changes to precipitation are anticipated given changes to dynamics, as well as differences in the responses of individual forest domains to changes in evapotranspiration (Kooperman et al., 2018) and differences in moisture recycling rates (Baker and Spracklen, 2022; Dyer et al., 2017). Figure 8 summarises the annual and seasonal changes to rainfall arising from our plausible global-scale forestation scenario, globally and in the tropical domains. Spatially distributed annual changes in 2095 are shown in Fig. S10.

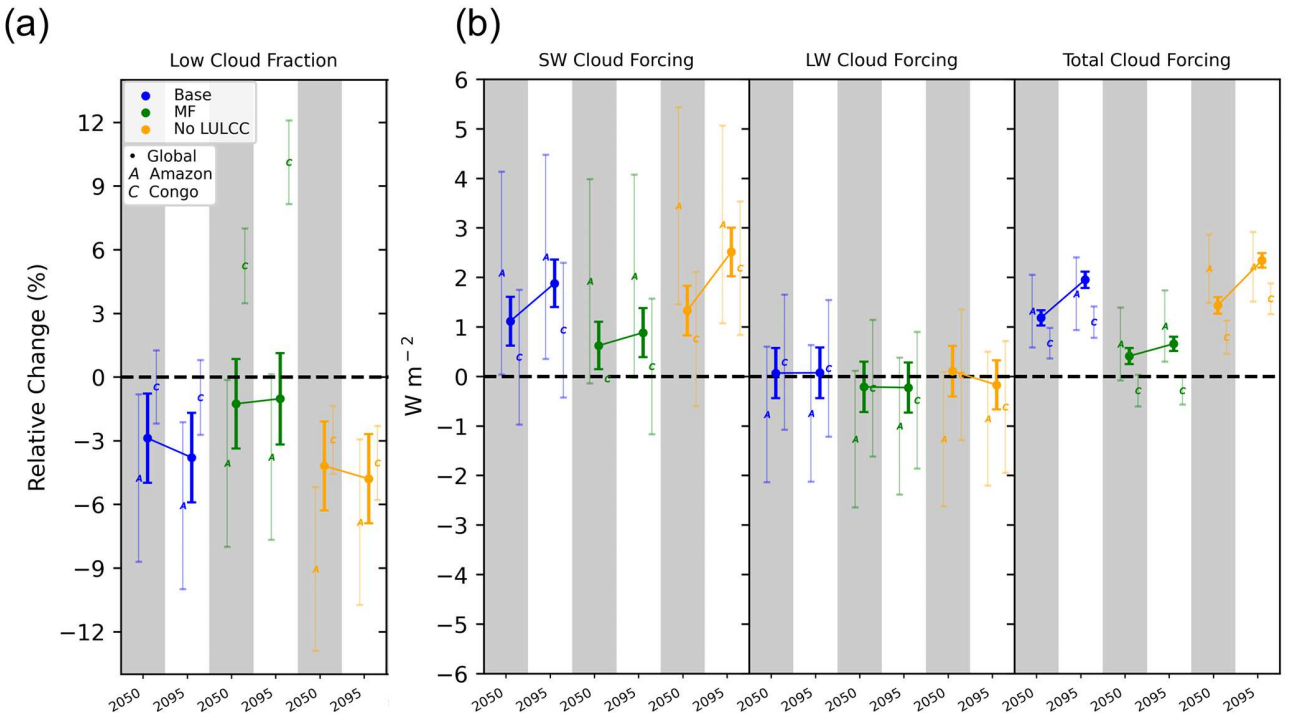

Figure 7. As Fig. 2b but showing differences in cloud cover integrated between 1200–700 hPa **(a)** and differences in clean-sky shortwave cloud radiative forcing, clean-sky longwave cloud radiative forcing, and total clean-sky cloud radiative forcing **(b)**.

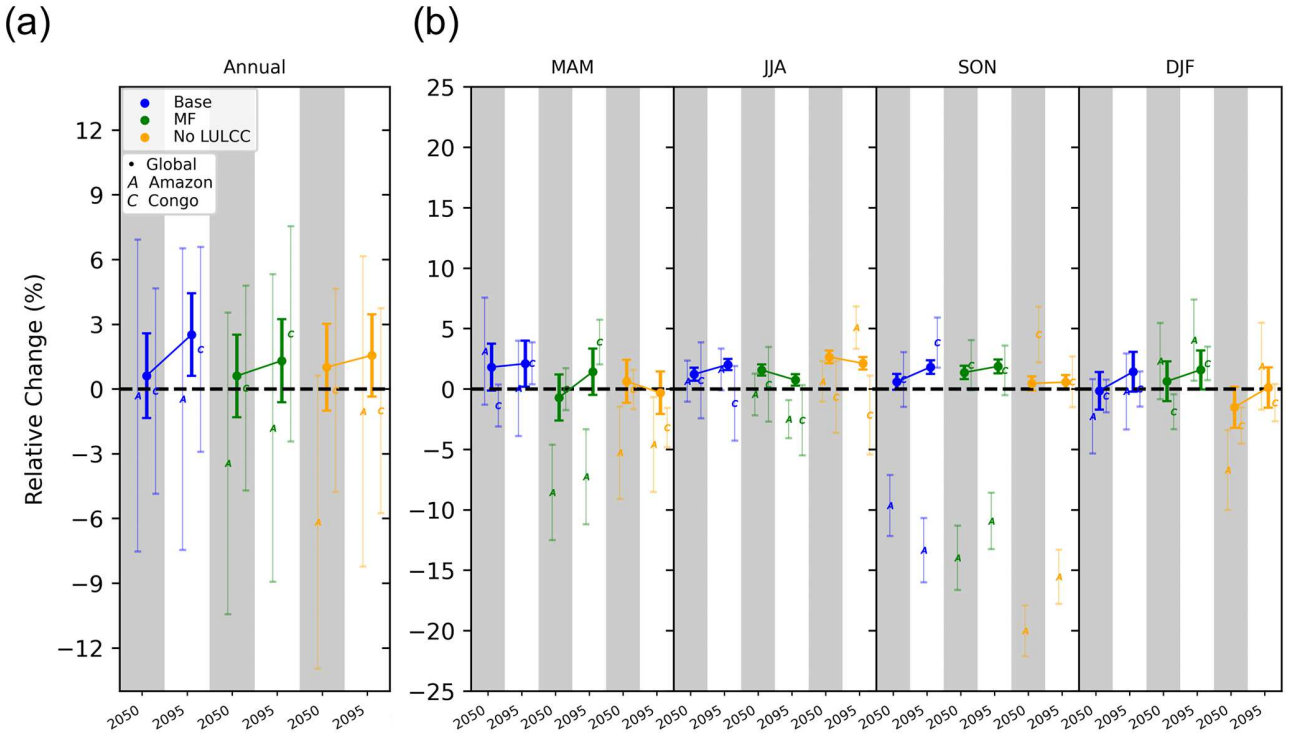

Figure 8. As Fig. 2b but showing differences in precipitation compared to 2020 between model experiments in the annual mean **(a)** and for each meteorological season **(b)**.

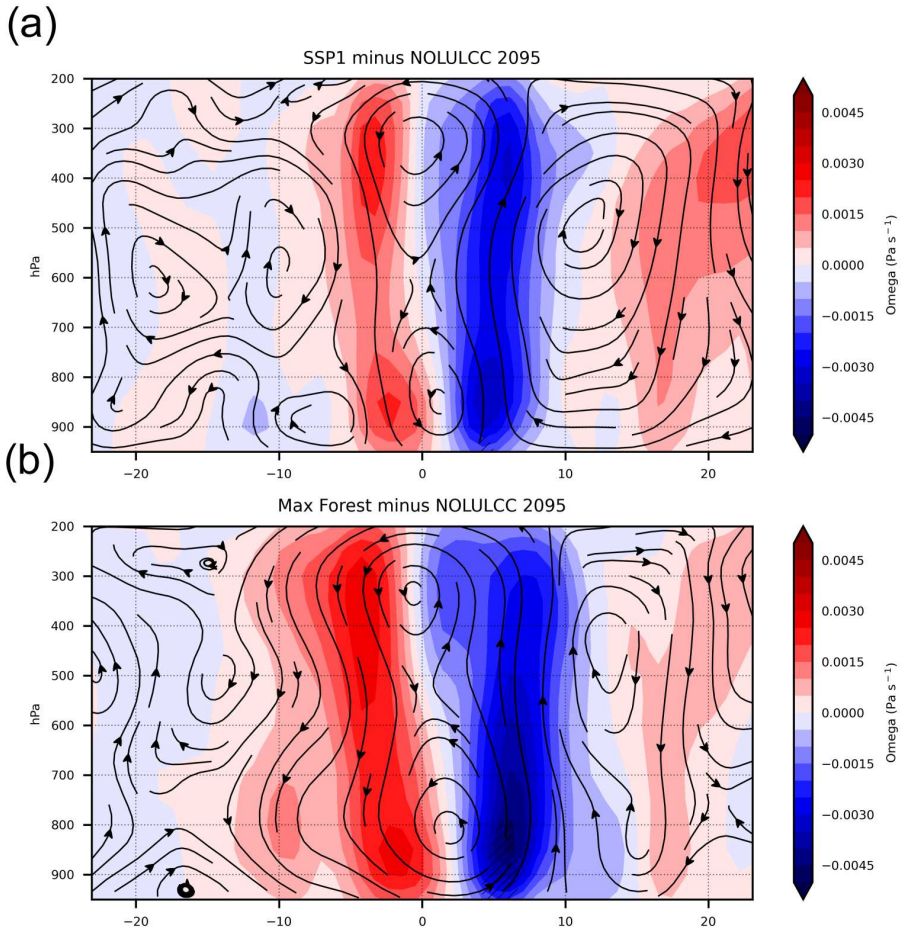

Figure 9. Differences in the Hadley circulation between scenarios at the end of the 21st century. Contour data are vertical velocity (omega); streamlines are the resultant vectors of omega × 1000 and meridional wind. Data are averaged over tropical latitudes.

Figures 8 and S10 demonstrate the impact on annual precipitation at 2050 and 2095 relative to the No LULCC scenario. We find large increases in precipitation over the Maritime Continent (albeit mostly over the ocean), decreases in the tropical Pacific relative to No LULCC in Max Forest, and increases and decreases on either side of the Equator relative to No LULCC in Base, resulting from a northward movement of the Intertropical Convergence Zone (ITCZ) (Fig. 9). There is little to no difference in precipitation over the Northern Hemisphere midlatitudes in either LULCC scenario (Fig. S10), reflecting the limited influence of convective rainfall (where land surface processes can have a direct influence) compared to large-scale frontal processes. The Max Forest scenario does show increases in precipitation of $\sim 0.5\,\mathrm{mm\,d^{-1}}$ over tropical Africa, Nepal, and parts of South America (Fig. S10), though these are not statistically significant at the 95 % confidence level. Significant changes in annual precipitation over land were also absent when the signal was decomposed into stratiform and convective components. However, substantial changes are observed in the precipitation signal when it is decomposed into meteorological seasons (Fig. 8). For example, globally, rainfall is higher over forested areas in the Max Forest scenario in Northern Hemisphere autumn (SON) compared to No LULCC, as well as in the Congo Basin in 2095 in spring (MAM – one of the region's rainy seasons). There are decreases in Max Forest Amazon Basin rainfall in MAM and SON but increases in DJF consistent with a shift in the ITCZ. Amazon Basin rainfall decreases in all scenarios in the autumn season (SON) in both 2050 and 2095.

The impact of the Max Forest scenario on annual precipitation over forested areas is not uniform across different regions. Trees are important in the maintenance of intensive tropical precipitation regimes via evapotranspiration and moisture recycling processes (C. Smith et al., 2023), but the extent of this influence depends on regional dynamics (Koopperman et al., 2018). The limited evapotranspiration (ET) increase in the Amazon Basin (Fig. 3) limits the local precipitation increase. In the Maritime Continent, ET changes are not significant, which leaves the precipitation signal to be determined by a northward shift of the ITCZ, itself less affected by discontinuities over land in this region compared to

the Amazon and Congo basins (Nicholson, 2018). Over the Congo Basin, the small but statistically significant increases in key parameters such as ET, latent heat flux, and convective cloud cover (Sect. 3.1 and 3.2) do not linearly translate into a significant annual precipitation increase, likely due to the region's complex dependency on moisture advection from remote sources (e.g. King et al., 2021; Munday et al., 2021) along with recycling (Dyer et al., 2017; Crowhurst et al., 2021). Trees directly influence atmospheric dynamics by increasing the roughness length compared to other, shorter vegetation types. The height at which momentum in a turbulent flow reaches zero is increased by up to 1 m in Max Forest relative to No LULCC, most prominently in tropical rainforests where canopy height is greatest (Fig. S7a). Forests thus act as a momentum sink for turbulent flows, and field experiments have shown pressure increases at grassland–forest margins when wind blows from a low-roughness grassland to a high-roughness forest as a result of the slowing effect of the transition to a higher roughness length (Nieveen et al., 2001). While such micrometeorological processes are necessarily highly parameterised in CESM2, it is interesting that our results show small increases in pressure reduced to sea level (SLP), particularly at the margins of the Congo Basin where the Max Forest scenario greatly expands tree cover into previously grassland environments (Fig. S7b). A small increase in surface pressure could potentially oppose increased rainfall drivers by reducing the increase in instability resulting from more evapotranspiration; however, a global model is not expected to be able to resolve these processes in detail (Fosser et al., 2015).

Model experiments with idealised forestation and deforestation scenarios have demonstrated the influence of trees on the general circulation (Portmann et al., 2022), in particular the Hadley cell, the dominant mean-state circulation feature in the tropics (Swann et al., 2012). This provides a mechanism by which land use change can affect climate remotely via teleconnection mechanisms analogous to those that drive the global climate response to internal variability modes such as ENSO (Boysen et al., 2020). Figure 9 illustrates the response of the Hadley circulation to the Base and Max Forest scenarios with respect to No LULCC by the end of the 21st century. In both scenarios, the response is characterised by a northward displacement of the ascending limb of the circulation with enhanced ascent (negative omega change) and a corresponding increase in descent (positive omega change) immediately south of the Equator. This results from changes to the hemispheric energy gradient due to Northern Hemisphere warming and ET increases (Laguë et al., 2019, 2021), in which the expected response in SSP1 is enhanced in Max Forest due to additional tree cover. The change here is consistent with the results of Portmann et al. (2022), who also used CESM2 to investigate the impacts of an idealised forestation scenario. However, with our land use change scenario, the magnitude of the change is much smaller. The increasing ascent north of the Equator, associated with forest expansion, is only statistically significant below 900 hPa in Base vs. No LULCC (Fig. 9); it is both stronger and more significant further into the troposphere (up to 800 hPa) in Max Forest vs. No LULCC. Figure 9 thus shows how Max Forest enhances the existing Hadley circulation response from the moderate forest expansion in the SSP1 scenario, with implications for future climate in the tropics including shifts in the locations and seasonality of convection and subsidence.

4 Discussion

In this study, we apply a global afforestation, reforestation, and forest restoration scenario within a greenhouse gas concentration scenario which is compatible with the temperature goals of the Paris Agreement. We demonstrate that, in this scenario, forest expansion increases evapotranspiration and latent heat flux while increasing water demand at the land surface and decreasing soil moisture and water supply as a result. The scenario avoids planting trees on croplands, urban regions, and protected conservation areas; consequently, about 50 % of the forest expansion occurs at the expense of grasslands (Parr et al., 2024) and other non-forest biomes. Since the demands for water and nutrients from trees are so much greater than those of grasses, especially during the transition from saplings to mature trees which occurs on the timescales of our model experiments, our results underline the importance of considering the long-term viability of trees as a climate change mitigation strategy (Hoek van Dijke et al., 2022). Our scenario attempts only to plant trees in climatically suitable locations, but as we impose land use change, we do not realistically represent tree mortality or the long-term viability of our expanded forest areas. This is particularly relevant for forest expansion schemes in the tropics, where most of the increased tree cover in both the Max Forest scenario and the global restoration commitments is undertaken and where biophysical benefits suggest forests can be most beneficial for climate change mitigation (Bala et al., 2007). We also do not consider the role of fire or other vegetation disturbances, such as herbivory, pests, and disease. These may dampen the potential of forestation efforts to mitigate climate change and have important implications for future climate and air quality in a warmer world with more trees, especially given that trees under conditions of water and heat stress are more vulnerable to disease, and climate change is anticipated to increase the range of various tree disease vectors. Evaluating the fire implications of forest expansion under future climates in particular should be a research priority and will be the focus of future work.

The viability of global-scale forest expansion will depend upon water availability, among other needs. In this sense afforestation has greater risks than reforestation and forest restoration, since the increase in water and nutrient demand is greater. There is a large spread across the CMIP6 ensemble in terms of simulation of tropical rainfall; while CESM2

is improved in this regard relative to previous versions of the model (Danabasoglu et al., 2020) and performs well relative to other CMIP6 models (Lee and Wang, 2021), the future trajectory of rainfall in tropical rainforests is still uncertain. For example, while the CMIP6 ensemble generally projects precipitation increases over the Congo Basin (Dosio et al., 2021) and decreases over the Amazon Basin (Parsons, 2020) under higher warming scenarios, the ability of models to simulate present-day tropical rainfall is extremely variable (Dosio et al., 2021), and trends under the lower SSP1-2.6 scenario used here are small. We note that an increase in the magnitude of the seasonal cycle of precipitation has been observed in the Amazon Basin in recent decades, with limited interannual change (Liang et al., 2020) but more extensive droughts (Marengo et al., 2018). Our results indicate that precipitation increases may result from forest expansion in the Congo Basin, primarily in the spring rainy season but that the potential for increased Amazon Basin rainfall in some seasons is not sufficient to counteract decreases in other seasons; in the case of the Amazon Basin, forest expansion does not prevent the future tendency towards drying or enhancement of the seasonal precipitation cycle. Model differences in land surface–atmosphere coupling likely reflect different approaches to parameterising processes at subgrid scales (Crowhurst et al., 2020). Our results have important implications for planning reforestation, afforestation, and forest enhancement because of the water demand increases, and we encourage similar studies using different Earth system models given the uncertainty in tropical precipitation simulation. Recent work has shown saturation of global water use efficiency since 2001 (Li et al., 2023) despite increases in evapotranspiration over the same time period (Yang et al., 2023), which highlights the importance of considering soil water demands in the terrestrial biosphere from a CDR perspective and may limit the future effectiveness of evapotranspiration-driven surface cooling mechanisms. Further, the increase in total evapotranspiration resulting from forest expansion is constrained by the decreasing soil evaporation resulting from reductions in soil moisture and increased shading of the surface, which act to partially offset increases in transpiration driven by higher NPP (Fig. S9). Combined with the decreases in stomatal conductance due to elevated CO_2 concentrations in future, which would tend to reduce evapotranspiration, there is not as strong an effect on evapotranspiration from Max Forest as might initially be anticipated from the increases in tropical tree cover (Fig. S9). The stomatal conductance effect would be more pronounced at higher CO_2 concentrations, and further work could explore this using other SSP GHG scenarios; indeed, a recent modelling study suggested that the negative impacts on Amazon Basin rainfall of deforestation and elevated CO_2 concentrations are broadly comparable (Sampaio et al., 2021). Additional important land processes resulting from forestation include changes to soil organic matter, which is significantly increased in Max Forest compared to No LULCC as forest soils generally store more carbon than the grassland or shrubland soils they are replacing. While this might be expected to increase soil moisture retention, alongside the greater potential for plant water storage in tree roots compared to grasses, the total grid-cell water storage (not shown) is still lower in key forest expansion regions in Max Forest, showing the dominance of the largely leaf-level increases in water demand in driving total water availability. Changes to soil infiltration are limited and not uniform in direction in afforested regions, showing the importance of rainfall and background soil moisture, and we encourage evaluation of CLM5's ability to simulate the relationship between soil carbon and hydrology (e.g. Telteu et al., 2021), especially in the tropics, as a result of PFT-level change.

While the Max Forest scenario expands forest area in both the Amazon Basin and the Congo Basin at similar rates, it is in the Congo Basin where the most significant impacts on the land surface and clouds are seen. This is an important result given recent work highlighting the differences in moisture recycling between the two rainforest basins in CMIP6 models (Baker and Spracklen, 2022); generally speaking, models capture moisture recycling in the Congo Basin well but underestimate it in the Amazon Basin, leading to an undersensitivity of Amazon Basin climate to LULCC. Our model runs showed large SST variability in the tropical Pacific that may have obscured LULCC-driven changes to the Amazon Basin hydroclimate; while this could be resolved with more ensemble members and/or a multi-model approach, the findings of Baker and Spracklen (2022) suggest this would not fully capture the sensitivity of the Amazonian climate to LULCC. Our results showing changes to cloud cover and convection over the Congo Basin may, therefore, also apply to the Amazon Basin; high recycling rates in the Amazon and Congo basins would suggest an increase in ET should drive an increase in precipitation, whereas lower rates in the Maritime Continent would result in less direct influence over land, notwithstanding the potential underestimation of Amazon Basin recycling rates in ESMs (Kooperman et al., 2018). Global-scale modelling suggests that deforestation can decrease cloud cover (Hua et al., 2023), but observational studies disagree on the impacts (Xu et al., 2022; Duveiller et al., 2021). De Hertog et al. (2024) found that ESMs generally responded to a fully afforested surface with a precipitation increase, but the extent of this was model-dependent with CESM2 showing a smaller precipitation response than MPI-ESM owing to lower rates of moisture recycling.

A process chain is expected from increased latent heat flux, LWP, and cloud cover, to changes in rainfall and aspects of the general circulation (Swann et al., 2012; Portmann et al., 2022). A change in the hemispheric energy gradient resulting from forest expansion in the Northern Hemisphere, where most of the land is, drives movement of the Hadley circulation towards the warmer hemisphere (Swann et al., 2012; Laguë et al., 2021). While we see some changes to this effect, their magnitude is relatively small. There is a balance to

be struck when designing model experiments to investigate the climate impacts of LULCC between using idealised scenarios to elucidate fundamental processes (Portmann et al., 2022; De Hertog et al., 2024) and scenarios that reflect actual LULCC trends or proposals (Swann et al., 2015). In policy-relevant scenarios, the signals are likely to be smaller given the limited impact of such LULCC in a world where changes to atmospheric dynamics will be dominated by warming, the Clausius–Clapeyron effect, and SST pattern change. Nevertheless, our results do suggest some impact of forest expansion on low cloud cover, which has a negative cloud radiative effect and cools the surface, particularly in the tropics where evaporative cooling also becomes significant. Enhancements in the strength of the tropical circulation might also affect cloud cover over land in Africa. This is in line with the mechanism proposed by Duveiller et al. (2021) based on observations. Additionally, the ability of trees to cool the surface via evapotranspiration is clear in the tropics, but we do not simulate a significant effect in the midlatitudes, which has recently been proposed as a cooling mechanism in the eastern USA (Barnes et al., 2024). However, we do not see the impacts on rainfall that might be expected given increased cloud cover and CCN. This result is the reverse of that found by Swann et al. (2015) in a study modelling realistic deforestation in the Amazon Basin. Swann et al. (2015) found that the LULCC influence on rainfall was small because of the already high levels of instability and convective rainfall found in the Amazon Basin. In our model, increases in clouds, cloud water, and CCN are only especially significant in tropical rainforests where these quantities are already very high. No significant differences in convective cloud at the conventional 95 % confidence level were found over tropical South America, and increases over the tropical western Pacific occurred mostly in the mid-troposphere, with commensurate decreases over the tropical eastern Pacific implying a change to the Pacific branch of the Walker Circulation. However, the lack of corresponding changes to convective cloud over tropical land suggests that this effect is not directly due to forest expansion in our scenario; Walker Circulation representation in global climate models is in any case highly uncertain (Chadwick et al., 2013; King and Washington, 2021). We encourage the use of high-resolution multi-scale Earth system modelling, such as the newly developed MUSICA configuration of CESM2 (Pfister et al., 2020), to explore LULCC–climate interactions in more detail, combining high-resolution dynamics and sophisticated atmospheric chemistry in a fully coupled model. It would also be useful to examine the sensitivity of different convection parameterisations to increased forest cover when combined with chemistry schemes, given the impacts from both increased evapotranspiration and increased CCN that result.

5 Conclusions

We used CESM2 to evaluate the global and regional hydroclimatic impacts of a global forestation scenario. We found a surface cooling due to increased evapotranspiration in the tropics which outweighed albedo-driven warming. No significant temperature effect was found in temperate forestation regions. Plant water demand increased significantly as a result of afforestation which shifted grassland to forest, driving strong decreases in soil moisture across domains as well as decreasing water availability. These decreases were not offset by water savings from stomatal closure under the moderate CO_2 increases of our scenario. Such changes in water dynamics may pose challenges for regions already susceptible to water scarcity. Additionally, the reduced water availability could impact agriculture and food production, particularly in areas where these sectors rely heavily on groundwater and rivers. In the atmosphere, increases in low cloud were simulated over some, primarily tropical, domains, with a decrease in the magnitude of the cloud radiative effect. Concentrations of cloud condensation nuclei increased over the expanded forests, while small but significant increases in cloud water and convective cloud cover occurred over tropical Africa. However, overall there was little annual precipitation change over land as a result of the LULCC. This was likely due to a combination of factors: the increase in plant transpiration was partially offset by decreasing evaporation from soil; increases in the local drivers of precipitation were small and localised over tropical rainforests, where their magnitude was already very large; the signal from the LULCC was small compared to that from the background warming scenario and SST change; the representation of tropical rainfall and land surface–atmosphere coupling in the model is limited by parameterisation of subgrid processes; and changes to surface winds from increasing roughness can result in surface pressure increases. We found a northward shift of the Hadley circulation, in line with similar studies using more idealised LULCC, suggesting an impact of forest cover on large-scale atmospheric circulation. However, this did not have a significant impact on rainfall over land. Our results suggest that when combined with GHG emissions reductions in a Paris-compatible world, CDR-focused global-scale forest expansion has the potential to deliver substantial climate change mitigation benefits without significantly disrupting global hydroclimate. However, the regional impacts on soil moisture and water availability are of vital importance when planning any kind of forest-based CDR and could hinder climate change mitigation efforts if they are not given sufficient consideration.

Code availability. The CESM2 model code is freely available online and can be downloaded from https://github.com/ESCOMP/CESM/tree/release-cesm2.1.3 (Danabasoglu et al., 2020). Python scripts used in the preparation of the figures are available from the lead author on request.

Data availability. The output from the CESM2 model experiments used in the analysis and the land use change data for each scenario are freely available in the following repositories: input data (https://doi.org/10.5281/zenodo.10782834, King, 2024a), land output data (https://doi.org/10.5281/zenodo.10797041, King, 2024b), and atmosphere output data (https://doi.org/10.5281/zenodo.10797083, King, 2024c, https://doi.org/10.5281/zenodo.10797087, King, 2024d, https://doi.org/10.5281/zenodo.10797092, King, 2024e).

Supplement. The supplement related to this article is available online at: https://doi.org/10.5194/bg-21-3883-2024-supplement.

Author contributions. JAK and MVM conceived the study with input from JW, PL, and ALSS. PL and SR developed the Max Forest scenario. JAK designed and performed model experiments, analysed the outputs, and wrote the original draft. JW, MVM, ALSS, and SR contributed to the development of the manuscript. MVM provided project funding.

Competing interests. James A. King is on the advisory panel for Ecologi, an organisation that invests in ecosystem restoration projects.

Disclaimer. Publisher's note: Copernicus Publications remains neutral with regard to jurisdictional claims made in the text, published maps, institutional affiliations, or any other geographical representation in this paper. While Copernicus Publications makes every effort to include appropriate place names, the final responsibility lies with the authors.

Acknowledgements. Model experiments were performed on the UK National Supercomputing Service ARCHER2. We thank Wuhu Feng, Chris Symonds, Grenville Lister, and Michael Mineter for technical support on ARCHER2. Data analysis was performed using JASMIN, the UK's collaborative data analysis environment. We acknowledge the support of the NCAR Land Model Working Group (LMWG) and Atmospheric Chemistry Observations and Modelling Group (ACOM). We also thank Simone Tilmes and Adam Herrington (NCAR) and Daniel Grosvenor (University of Leeds) for helpful comments.

Financial support. This research has been supported by a United Kingdom Research and Innovation (UKRI) Future Leaders Fellowship award (grant no. MR/T019867/1) and the US Department of Energy Office of Biological and Environmental Research Regional and Global Model Analysis Program (grant no. DE-SC0021209).

Review statement. This paper was edited by Anja Rammig and reviewed by two anonymous referees.

References

Abiodun, B. J., Salami, A. T., Matthew, O. J., and Odedokun, S.: Potential impacts of afforestation on climate change and extreme events in Nigeria, Clim. Dynam., 41, 277–293, https://doi.org/10.1007/S00382-012-1523-9, 2013.

Alkama, R. and Cescatti, A.: Biophysical climate impacts of recent changes in global forest cover, Science, 351, 600–604, https://doi.org/10.1126/SCIENCE.AAC8083, 2016.

Baker, J. C. A. and Spracklen, D. V.: Divergent Representation of Precipitation Recycling in the Amazon and the Congo in CMIP6 Models, Geophys. Res. Lett., 49, e2021GL095136, https://doi.org/10.1029/2021GL095136, 2022.

Bala, G., Caldeira, K., Wickett, M., Phillips, T. J., Lobell, D. B., Delire, C., and Mirin, A.: Combined climate and carbon-cycle effects of large-scale deforestation, P. Natl. Acad. Sci. USA, 104, 6550–6555, https://doi.org/10.1073/PNAS.0608998104, 2007.

Barnes, M. L., Zhang, Q., Robeson, S. M., Young, L., Burakowski, E. A., Oishi, A. C., Stoy, P. C., Katul, G., and Novick, K. A.: A Century of Reforestation Reduced Anthropogenic Warming in the Eastern United States, Earths Future, 12, e2023EF003663, https://doi.org/10.1029/2023EF003663, 2024.

Bastin, J. F., Finegold, Y., Garcia, C., Mollicone, D., Rezende, M., Routh, D., Zohner, C. M., and Crowther, T. W.: The global tree restoration potential, Science, 364, 76–79, https://doi.org/10.1126/science.aax0848, 2019.

Bekenshtein, R., Price, C., and Mareev, E.: Is Amazon deforestation decreasing the number of thunderstorms over South America?, Q. J. Roy. Meteor. Soc., 149, 2514–2526, https://doi.org/10.1002/QJ.4518, 2023.

Bonan, G. B.: Forests and climate change: forcings, feedbacks, and the climate benefits of forests, Science, 320, 1444–1449, https://doi.org/10.1126/science.1155121, 2008.

Bonan, G. B.: Forests, Climate, and Public Policy: A 500-Year Interdisciplinary Odyssey, Annu. Rev. Ecol. Evol. S., 47, 97–121, https://doi.org/10.1146/annurev-ecolsys-121415-032359, 2016.

Bonan, G. B., Pollard, D., and Thompson, S. L.: Effects of boreal forest vegetation on global climate, Nature, 359, 716–718, https://doi.org/10.1038/359716a0, 1992.

Bond, W. J., Stevens, N., Midgley, G. F., and Lehmann, C. E. R.: The Trouble with Trees: Afforestation Plans for Africa, Trends Ecol. Evol., 34, 963–965, https://doi.org/10.1016/J.TREE.2019.08.003, 2019.

Boysen, L. R., Brovkin, V., Pongratz, J., Lawrence, D. M., Lawrence, P., Vuichard, N., Peylin, P., Liddicoat, S., Hajima, T., Zhang, Y., Rocher, M., Delire, C., Séférian, R., Arora, V. K., Nieradzik, L., Anthoni, P., Thiery, W., Laguë, M. M., Lawrence, D., and Lo, M.-H.: Global climate response to idealized deforestation in CMIP6 models, Biogeosciences, 17, 5615–5638, https://doi.org/10.5194/bg-17-5615-2020, 2020.

Chadwick, R., Boutle, I., and Martin, G.: Spatial Patterns of Precipitation Change in CMIP5: Why the Rich Do Not Get Richer in the Tropics, J. Climate, 26, 3803–3822, https://doi.org/10.1175/JCLI-D-12-00543.1, 2013.

Cook-Patton, S. C., Leavitt, S. M., Gibbs, D., Harris, N. L., Lister, K., Anderson-Teixeira, K. J., Briggs, R. D., Chazdon, R. L., Crowther, T. W., Ellis, P. W., Griscom, H. P., Herrmann, V., Holl, K. D., Houghton, R. A., Larrosa, C., Lomax, G., Lucas, R., Madsen, P., Malhi, Y., Paquette, A., Parker, J. D., Paul, K., Routh, D., Roxburgh, S., Saatchi, S., van den Hoogen, J., Walker, W. S., Wheeler, C. E., Wood, S. A., Xu, L., and Griscom, B. W.: Mapping carbon accumulation potential from global natural forest regrowth, Nature, 585, 545–550, https://doi.org/10.1038/s41586-020-2686-x, 2020.

Crowhurst, D., Dadson, S., Peng, J., and Washington, R.: Contrasting controls on Congo Basin evaporation at the two rainfall peaks, Clim. Dynam., 56, 1609–1624, https://doi.org/10.1007/S00382-020-05547-1, 2021.

Crowhurst, D. M., Dadson, S. J., and Washington, R.: Evaluation of Evaporation Climatology for the Congo Basin Wet Seasons in 11 Global Climate Models, J. Geophys. Res.-Atmos., 125, e2019JD030619, https://doi.org/10.1029/2019JD030619, 2020.

Danabasoglu, G., Bates, S. C., Briegleb, B. P., Jayne, S. R., Jochum, M., Large, W. G., Peacock, S., and Yeager, S. G.: The CCSM4 Ocean Component, J. Climate, 25, 1361–1389, https://doi.org/10.1175/JCLI-D-11-00091.1, 2012.

Danabasoglu, G., Lamarque, J. F., Bacmeister, J., Bailey, D. A., DuVivier, A. K., Edwards, J., Emmons, L. K., Fasullo, J., Garcia, R., Gettelman, A., Hannay, C., Holland, M. M., Large, W. G., Lauritzen, P. H., Lawrence, D. M., Lenaerts, J. T. M., Lindsay, K., Lipscomb, W. H., Mills, M. J., Neale, R., Oleson, K. W., Otto-Bliesner, B., Phillips, A. S., Sacks, W., Tilmes, S., van Kampenhout, L., Vertenstein, M., Bertini, A., Dennis, J., Deser, C., Fischer, C., Fox-Kemper, B., Kay, J. E., Kinnison, D., Kushner, P. J., Larson, V. E., Long, M. C., Mickelson, S., Moore, J. K., Nienhouse, E., Polvani, L., Rasch, P. J., and Strand, W. G.: The Community Earth System Model Version 2 (CESM2), J. Adv. Model. Earth Sy., 12, e2019MS001916, https://doi.org/10.1029/2019MS001916, 2020 (code available at: https://github.com/ESCOMP/CESM/tree/release-cesm2.1.3, last access: 30 October 2023).

De Hertog, S. J., Lopez-Fabara, C. E., van der Ent, R., Keune, J., Miralles, D. G., Portmann, R., Schemm, S., Havermann, F., Guo, S., Luo, F., Manola, I., Lejeune, Q., Pongratz, J., Schleussner, C.-F., Seneviratne, S. I., and Thiery, W.: Effects of idealized land cover and land management changes on the atmospheric water cycle, Earth Syst. Dynam., 15, 265–291, https://doi.org/10.5194/esd-15-265-2024, 2024.

De Wit, H. A., Bryn, A., Hofgaard, A., Karstensen, J., Kvalevåg, M. M., and Peters, G. P.: Climate warming feedback from mountain birch forest expansion: reduced albedo dominates carbon uptake, Glob. Change Biol., 20, 2344–2355, https://doi.org/10.1111/GCB.12483, 2014.

Dosio, A., Jury, M. W., Almazroui, M., Ashfaq, M., Diallo, I., Engelbrecht, F. A., Klutse, N. A. B., Lennard, C., Pinto, I., Sylla, M. B., and Tamoffo, A. T.: Projected future daily characteristics of African precipitation based on global (CMIP5, CMIP6) and regional (CORDEX, CORDEX-CORE) climate models, Clim. Dynam., 57, 3135–3158, https://doi.org/10.1007/s00382-021-05859-w, 2021.

Drever, C. R., Cook-Patton, S. C., Akhter, F., Badiou, P. H., Chmura, G. L., Davidson, S. J., Desjardins, R. L., Dyk, A., Fargione, J. E., Fellows, M., Filewod, B., Hessing-Lewis, M., Jayasundara, S., Keeton, W. S., Kroeger, T., Lark, T. J., Le, E., Leavitt, S. M., LeClerc, M. E., Lemprière, T. C., Metsaranta, J., McConkey, B., Neilson, E., St-Laurent, G. P., Puric-Mladenovic, D., Rodrigue, S., Soolanayakanahally, R. Y., Spawn, S. A., Strack, M., Smyth, C., Thevathasan, N., Voicu, M., Williams, C. A., Woodbury, P. B., Worth, D. E., Xu, Z., Yeo, S., and Kurz, W. A.: Natural climate solutions for Canada, Sci. Adv., 7, eabd6034, https://doi.org/10.1126/sciadv.abd6034, 2021.

Duveiller, G., Filipponi, F., Ceglar, A., Bojanowski, J., Alkama, R., and Cescatti, A.: Revealing the widespread potential of forests to increase low level cloud cover, Nat. Commun., 12, 1–15, https://doi.org/10.1038/s41467-021-24551-5, 2021.

Dyer, E. L. E., Jones, D. B. A., Nusbaumer, J., Li, H., Collins, O., Vettoretti, G., and Noone, D.: Congo Basin precipitation: Assessing seasonality, regional interactions, and sources of moisture, J. Geophys. Res.-Atmos., 122, 6882–6898, https://doi.org/10.1002/2016JD026240, 2017.

Emmons, L. K., Schwantes, R. H., Orlando, J. J., Tyndall, G., Kinnison, D., Lamarque, J. F., Marsh, D., Mills, M. J., Tilmes, S., Bardeen, C., Buchholz, R. R., Conley, A., Gettelman, A., Garcia, R., Simpson, I., Blake, D. R., Meinardi, S., and Pétron, G.: The Chemistry Mechanism in the Community Earth System Model Version 2 (CESM2), J. Adv. Model. Earth Sy., 12, e2019MS001882, https://doi.org/10.1029/2019MS001882, 2020.

Fankhauser, S., Smith, S. M., Allen, M., Axelsson, K., Hale, T., Hepburn, C., Kendall, J. M., Khosla, R., Lezaun, J., Mitchell-Larson, E., Obersteiner, M., Rajamani, L., Rickaby, R., Seddon, N., and Wetzer, T.: The meaning of net zero and how to get it right, Nat. Clim. Change, 12, 15–21, https://doi.org/10.1038/s41558-021-01245-w, 2021.

Fleischman, F., Basant, S., Chhatre, A., Coleman, E. A., Fischer, H. W., Gupta, D., Güneralp, B., Kashwan, P., Khatri, D., Muscarella, R., Powers, J. S., Ramprasad, V., Rana, P., Solorzano, C. R., and Veldman, J. W.: Pitfalls of Tree Planting Show Why We Need People-Centered Natural Climate Solutions, BioScience, 70, 947–950, https://doi.org/10.1093/BIOSCI/BIAA094, 2020.

Fosser, G., Khodayar, S., and Berg, P.: Benefit of convection permitting climate model simulations in the representation of convective precipitation, Clim. Dynam., 44, 45–60, https://doi.org/10.1007/S00382-014-2242-1, 2015.

Friedlingstein, P., Allen, M., Canadell, J. G., Peters, G. P., and Seneviratne, S. I.: Comment on "The global tree restoration potential," Science, 366, 76–79, https://doi.org/10.1126/science.aay8060, 2019.

Fuhrman, J., McJeon, H., Patel, P., Doney, S. C., Shobe, W. M., and Clarens, A. F.: Food–energy–water implications of negative emissions technologies in a +1.5 °C future, Nat. Clim. Change, 10, 920–927, https://doi.org/10.1038/s41558-020-0876-z, 2020.

Gidden, M. J., Riahi, K., Smith, S. J., Fujimori, S., Luderer, G., Kriegler, E., van Vuuren, D. P., van den Berg, M., Feng, L., Klein, D., Calvin, K., Doelman, J. C., Frank, S., Fricko, O., Harmsen, M., Hasegawa, T., Havlik, P., Hilaire, J., Hoesly, R., Horing, J., Popp, A., Stehfest, E., and Takahashi, K.: Global

emissions pathways under different socioeconomic scenarios for use in CMIP6: a dataset of harmonized emissions trajectories through the end of the century, Geosci. Model Dev., 12, 1443–1475, https://doi.org/10.5194/gmd-12-1443-2019, 2019.

Girardin, C. A. J., Jenkins, S., Seddon, N., Allen, M., Lewis, S. L., Wheeler, C. E., Griscom, B. W., and Malhi, Y.: Nature-based solutions can help cool the planet—if we act now, Nature, 593, 191–194, https://doi.org/10.1038/d41586-021-01241-2, 2021.

Grassi, G., House, J., Dentener, F., Federici, S., Den Elzen, M., and Penman, J.: The key role of forests in meeting climate targets requires science for credible mitigation, Nat. Clim. Change, 7, 220–226, https://doi.org/10.1038/nclimate3227, 2017.

Griscom, B. W., Adams, J., Ellis, P. W., Houghton, R. A., Lomax, G., Miteva, D. A., Schlesinger, W. H., Shoch, D., Siikamäki, J. V., Smith, P., Woodbury, P., Zganjar, C., Blackman, A., Campari, J., Conant, R. T., Delgado, C., Elias, P., Gopalakrishna, T., Hamsik, M. R., Herrero, M., Kiesecker, J., Landis, E., Laestadius, L., Leavitt, S. M., Minnemeyer, S., Polasky, S., Potapov, P., Putz, F. E., Sanderman, J., Silvius, M., Wollenberg, E., and Fargione, J.: Natural climate solutions, P. Natl. Acad. Sci. USA, 114, 11645–11650, https://doi.org/10.1073/pnas.1710465114, 2017.

Guenther, A. B., Jiang, X., Heald, C. L., Sakulyanontvittaya, T., Duhl, T., Emmons, L. K., and Wang, X.: The Model of Emissions of Gases and Aerosols from Nature version 2.1 (MEGAN2.1): an extended and updated framework for modeling biogenic emissions, Geosci. Model Dev., 5, 1471–1492, https://doi.org/10.5194/gmd-5-1471-2012, 2012.

Heald, C. L. and Spracklen, D. V.: Land Use Change Impacts on Air Quality and Climate, Chem. Rev., 115, 4476–4496, https://doi.org/10.1021/cr500446g, 2015.

Hoek van Dijke, A. J., Herold, M., Mallick, K., Benedict, I., Machwitz, M., Schlerf, M., Pranindita, A., Theeuwen, J. J. E., Bastin, J. F., and Teuling, A. J.: Shifts in regional water availability due to global tree restoration, Nat. Geosci. 2022 155, 15, 363–368, https://doi.org/10.1038/s41561-022-00935-0, 2022.

Hoesly, R. M., Smith, S. J., Feng, L., Klimont, Z., Janssens-Maenhout, G., Pitkanen, T., Seibert, J. J., Vu, L., Andres, R. J., Bolt, R. M., Bond, T. C., Dawidowski, L., Kholod, N., Kurokawa, J.-I., Li, M., Liu, L., Lu, Z., Moura, M. C. P., O'Rourke, P. R., and Zhang, Q.: Historical (1750–2014) anthropogenic emissions of reactive gases and aerosols from the Community Emissions Data System (CEDS), Geosci. Model Dev., 11, 369–408, https://doi.org/10.5194/gmd-11-369-2018, 2018.

Hua, W., Zhou, L., Dai, A., Chen, H., and Liu, Y.: Important non-local effects of deforestation on cloud cover changes in CMIP6 models, Environ. Res. Lett., 18, 094047, https://doi.org/10.1088/1748-9326/ACF232, 2023.

IPCC: Global Warming of 1.5°C, Cambridge University Press, https://doi.org/10.1017/9781009157940, 2022.

Kennedy, D., Swenson, S., Oleson, K. W., Lawrence, D. M., Fisher, R., Lola da Costa, A. C., and Gentine, P.: Implementing Plant Hydraulics in the Community Land Model, Version 5, J. Adv. Model. Earth Sy., 11, 485–513, https://doi.org/10.1029/2018MS001500, 2019.

King, J. A.: CESM2 land use data for study on hydrological impacts of large-scale forest expansion, Zenodo [data set], https://doi.org/10.5281/zenodo.10782834, 2024a.

King, J. A.: CESM2 land output data for study on hydrological impacts of large-scale forest expansion, Zenodo [data set], https://doi.org/10.5281/zenodo.10797041, 2024b.

King, J. A.: CESM2 atmosphere output data for study on hydrological impacts of large-scale forest expansion, Zenodo [data set], https://doi.org/10.5281/zenodo.10797083, 2024c.

King, J. A.: CESM2 atmosphere output data for study on hydrological impacts of large-scale forest expansion, Zenodo [data set], https://doi.org/10.5281/zenodo.10797087, 2024d.

King, J. A.: CESM2 atmosphere output data for study on hydrological impacts of large-scale forest expansion, Zenodo [data set], https://doi.org/10.5281/zenodo.10797092, 2024e.

King, J. A. and Washington, R.: Future Changes in the Indian Ocean Walker Circulation and Links to Kenyan Rainfall, J. Geophys. Res.-Atmos., 126, e2021JD034585, https://doi.org/10.1029/2021JD034585, 2021.

King, J. A., Engelstaedter, S., Washington, R., and Munday, C.: Variability of the Turkana Low-Level Jet in Reanalysis and Models: Implications for Rainfall, J. Geophys. Res.-Atmos., 126, e2020JD034154, https://doi.org/10.1029/2020JD034154, 2021.

Kirschbaum, M. U. F., Whitehead, D., Dean, S. M., Beets, P. N., Shepherd, J. D., and Ausseil, A.-G. E.: Implications of albedo changes following afforestation on the benefits of forests as carbon sinks, Biogeosciences, 8, 3687–3696, https://doi.org/10.5194/bg-8-3687-2011, 2011.

Kok, M. T. J., Meijer, J. R., van Zeist, W.-J., Hilbers, J. P., Immovilli, M., Janse, J. H., Stehfest, E., Bakkenes, M., Tabeau, A., Schipper, A. M., and Alkemade, R.: Assessing ambitious nature conservation strategies in a below 2-degree and food-secure world, Biol. Conserv., 284, 110068, https://doi.org/10.1016/J.BIOCON.2023.110068, 2023.

Kooperman, G. J., Chen, Y., Hoffman, F. M., Koven, C. D., Lindsay, K., Pritchard, M. S., Swann, A. L. S., and Randerson, J. T.: Forest response to rising CO_2 drives zonally asymmetric rainfall change over tropical land, Nat. Clim. Change, 2018 85, 8, 434–440, https://doi.org/10.1038/s41558-018-0144-7, 2018.

Laguë, M. M., Bonan, G. B., and Swann, A. L. S.: Separating the Impact of Individual Land Surface Properties on the Terrestrial Surface Energy Budget in both the Coupled and Uncoupled Land–Atmosphere System, J. Climate, 32, 5725–5744, https://doi.org/10.1175/JCLI-D-18-0812.1, 2019.

Laguë, M. M., Swann, A. L. S., and Boos, W. R.: Radiative Feedbacks on Land Surface Change and Associated Tropical Precipitation Shifts, J. Climate, 34, 6651–6672, https://doi.org/10.1175/JCLI-D-20-0883.1, 2021.

Lawrence, D., Coe, M., Walker, W., Verchot, L., and Vandecar, K.: The Unseen Effects of Deforestation: Biophysical Effects on Climate, Front. For. Glob. Chang., 5, 756115, https://doi.org/10.3389/FFGC.2022.756115, 2022.

Lawrence, D. M., Hurtt, G. C., Arneth, A., Brovkin, V., Calvin, K. V., Jones, A. D., Jones, C. D., Lawrence, P. J., de Noblet-Ducoudré, N., Pongratz, J., Seneviratne, S. I., and Shevliakova, E.: The Land Use Model Intercomparison Project (LUMIP) contribution to CMIP6: rationale and experimental design, Geosci. Model Dev., 9, 2973–2998, https://doi.org/10.5194/gmd-9-2973-2016, 2016.

Lawrence, D. M., Fisher, R. A., Koven, C. D., Oleson, K. W., Swenson, S. C., Bonan, G., Collier, N., Ghimire, B., van Kampenhout, L., Kennedy, D., Kluzek, E., Lawrence, P. J., Li, F.,

Li, H., Lombardozzi, D., Riley, W. J., Sacks, W. J., Shi, M., Vertenstein, M., Wieder, W. R., Xu, C., Ali, A. A., Badger, A. M., Bisht, G., van den Broeke, M., Brunke, M. A., Burns, S. P., Buzan, J., Clark, M., Craig, A., Dahlin, K., Drewniak, B., Fisher, J. B., Flanner, M., Fox, A. M., Gentine, P., Hoffman, F., Keppel-Aleks, G., Knox, R., Kumar, S., Lenaerts, J., Leung, L. R., Lipscomb, W. H., Lu, Y., Pandey, A., Pelletier, J. D., Perket, J., Randerson, J. T., Ricciuto, D. M., Sanderson, B. M., Slater, A., Subin, Z. M., Tang, J., Thomas, R. Q., Val Martin, M., and Zeng, X.: The Community Land Model Version 5: Description of New Features, Benchmarking, and Impact of Forcing Uncertainty, J. Adv. Model. Earth Sy., 11, 4245–4287, https://doi.org/10.1029/2018MS001583, 2019.

Lawrence, M. G., Schäfer, S., Muri, H., Scott, V., Oschlies, A., Vaughan, N. E., Boucher, O., Schmidt, H., Haywood, J., and Scheffran, J.: Evaluating climate geoengineering proposals in the context of the Paris Agreement temperature goals, Nat. Commun. 9, 1–19, https://doi.org/10.1038/s41467-018-05938-3, 2018.

Lee, T.-H., Lo, M.-H., Chiang, C.-L., and Kuo, Y.-N.: The maritime continent's rainforests modulate the local interannual evapotranspiration variability, Commun. Earth Environ., 4, 1–7, https://doi.org/10.1038/s43247-023-01126-4, 2023.

Lee, Y. C. and Wang, Y. C.: Evaluating diurnal rainfall signal performance from cmip5 to cmip6, J. Climate, 34, 7607–7623, https://doi.org/10.1175/JCLI-D-20-0812.1, 2021.

Lewis, S. L., Mitchard, E. T. A., Prentice, C., Maslin, M., and Poulter, B.: Comment on "The global tree restoration potential," Science, 366, 1–3, https://doi.org/10.1126/SCIENCE.AAZ0388, 2019a.

Lewis, S. L., Wheeler, C. E., Mitchard, E. T. A., and Koch, A.: Restoring natural forests is the best way to remove atmospheric carbon, Nature, 568, 25–28, https://doi.org/10.1038/d41586-019-01026-8, 2019b.

Li, F., Xiao, J., Chen, J., Ballantyne, A., Jin, K., Li, B., Abraha, M., and John, R.: Global water use efficiency saturation due to increased vapor pressure deficit, Science, 381, 672–677, https://doi.org/10.1126/SCIENCE.ADF5041, 2023.

Liang, Y. C., Lo, M. H., Lan, C. W., Seo, H., Ummenhofer, C. C., Yeager, S., Wu, R. J., and Steffen, J. D.: Amplified seasonal cycle in hydroclimate over the Amazon river basin and its plume region, Nat. Commun., 11, 1–11, https://doi.org/10.1038/s41467-020-18187-0, 2020.

Liu, X., Ma, P.-L., Wang, H., Tilmes, S., Singh, B., Easter, R. C., Ghan, S. J., and Rasch, P. J.: Description and evaluation of a new four-mode version of the Modal Aerosol Module (MAM4) within version 5.3 of the Community Atmosphere Model, Geosci. Model Dev., 9, 505–522, https://doi.org/10.5194/gmd-9-505-2016, 2016.

Marengo, J. A., Souza, C. M., Thonicke, K., Burton, C., Halladay, K., Betts, R. A., Alves, L. M., and Soares, W. R.: Changes in Climate and Land Use Over the Amazon Region: Current and Future Variability and Trends, Front. Earth Sci., 6, 425317, https://doi.org/10.3389/FEART.2018.00228, 2018.

Martin, M. P., Woodbury, D. J., Doroski, D. A., Nagele, E., Storace, M., Cook-Patton, S. C., Pasternack, R., and Ashton, M. S.: People plant trees for utility more often than for biodiversity or carbon, Biol. Conserv., 261, 109224, https://doi.org/10.1016/J.BIOCON.2021.109224, 2021.

Mo, L., Zohner, C. M., Reich, P. B., Liang, J., de Miguel, S., Nabuurs, G.-J., Renner, S. S., van den Hoogen, J., Araza, A., Herold, M., Mirzagholi, L., Ma, H., Averill, C., Phillips, O. L., Gamarra, J. G. P., Hordijk, I., Routh, D., Abegg, M., Adou Yao, Y. C., Alberti, G., Almeyda Zambrano, A. M., Alvarado, B. V., Alvarez-Dávila, E., Alvarez-Loayza, P., Alves, L. F., Amaral, I., Ammer, C., Antón-Fernández, C., Araujo-Murakami, A., Arroyo, L., Avitabile, V., Aymard, G. A., Baker, T. R., Balazy, R., Banki, O., Barroso, J. G., Bastian, M. L., Bastin, J.-F., Birigazzi, L., Birnbaum, P., Bitariho, R., Boeckx, P., Bongers, F., Bouriaud, O., Brancalion, P. H. S., Brandl, S., Brearley, F. Q., Brienen, R., Broadbent, E. N., Bruelheide, H., Bussotti, F., Cazzolla Gatti, R., César, R. G., Cesljar, G., Chazdon, R. L., Chen, H. Y. H., Chisholm, C., Cho, H., Cienciala, E., Clark, C., Clark, D., Colletta, G. D., Coomes, D. A., Cornejo Valverde, F., Corral-Rivas, J. J., Crim, P. M., Cumming, J. R., Dayanandan, S., de Gasper, A. L., Decuyper, M., Derroire, G., DeVries, B., Djordjevic, I., Dolezal, J., Dourdain, A., Engone Obiang, N. L., Enquist, B. J., Eyre, T. J., Fandohan, A. B., Fayle, T. M., Feldpausch, T. R., Ferreira, L. V., Finér, L., Fischer, M., Fletcher, C., Frizzera, L., Gianelle, D., Glick, H. B., Harris, D. J., Hector, A., Hemp, A., Hengeveld, G., Hérault, B., Herbohn, J. L., Hillers, A., Honorio Coronado, E. N., Hui, C., Ibanez, T., Imai, N., et al.: Integrated global assessment of the natural forest carbon potential, Nature, 624, 92–101, https://doi.org/10.1038/s41586-023-06723-z, 2023.

Munday, C., Washington, R., and Hart, N.: African Low-Level Jets and Their Importance for Water Vapor Transport and Rainfall, Geophys. Res. Lett., 48, e2020GL090999, https://doi.org/10.1029/2020GL090999, 2021.

Nabuurs, G.-J. and R. Mrabet, A. Abu Hatab, M. Bustamante, H. Clark, P. Havlík, J. House, C. Mbow, K. N. Ninan, A. Popp, S. Roe, B. Sohngen, S. T.: IPCC Mitigation: Agriculture, Forestry and Other Land Uses, Clim. Chang. 2022 – Mitig. Clim. Chang., https://doi.org/10.1017/9781009157926.009, 747–860, 2023.

Nicholson, S. E.: The ITCZ and the Seasonal Cycle over Equatorial Africa, B. Am. Meteorol. Soc., 99, 337–348, https://doi.org/10.1175/BAMS-D-16-0287.1, 2018.

Nieveen, J. P., El-Kilani, R. M. M., and Jacobs, A. F. G.: Behaviour of the static pressure around a tussock grassland–forest interface, Agr. Forest Meteorol., 106, 253–259, https://doi.org/10.1016/S0168-1923(00)00234-3, 2001.

Nosetto, M. D., Jobbágy, E. G., and Paruelo, J. M.: Land-use change and water losses: the case of grassland afforestation across a soil textural gradient in central Argentina, Glob. Change Biol., 11, 1101–1117, https://doi.org/10.1111/J.1365-2486.2005.00975.X, 2005.

Orlov, A., Aunan, K., Mistry, M. N., Lejeune, Q., Pongratz, J., Thiery, W., Gasparrini, A., Reed, E. U., and Schleussner, C. F.: Neglected implications of land-use and land-cover changes on the climate-health nexus, Environ. Res. Lett., 18, 061005, https://doi.org/10.1088/1748-9326/ACD799, 2023.

Parr, C. L., Beest, M. te, and Stevens, N.: Conflation of reforestation with restoration is widespread, Science, 383, 698–701, https://doi.org/10.1126/SCIENCE.ADJ0899, 2024.

Parsons, L. A.: Implications of CMIP6 Projected Drying Trends for 21st Century Amazonian Drought Risk, Earths Future, 8, e2020EF001608, https://doi.org/10.1029/2020EF001608, 2020.

Pfister, G. G., Eastham, S. D., Arellano, A. F., Aumont, B., Barsanti, K. C., Barth, M. C., Conley, A., Davis, N. A., Emmons, L. K., Fast, J. D., Fiore, A. M., Gaubert, B., Goldhaber, S., Granier, C., Grell, G. A., Guevara, M., Henze, D. K., Hodzic, A., Liu, X., Marsh, D. R., Orlando, J. J., Plane, J. M. C., Polvani, L. M., Rosenlof, K. H., Steiner, A. L., Jacob, D. J., and Brasseur, G. P.: The Multi-Scale Infrastructure for Chemistry and Aerosols (MUSICA), B. Am. Meteorol. Soc., 101, E1743–E1760, https://doi.org/10.1175/BAMS-D-19-0331.1, 2020.

Portmann, R., Beyerle, U., Davin, E., Fischer, E. M., De Hertog, S., and Schemm, S.: Global forestation and deforestation affect remote climate via adjusted atmosphere and ocean circulation, Nat. Commun., 13, 1–11, https://doi.org/10.1038/s41467-022-33279-9, 2022.

Robinson, M. and Shine, T.: Achieving a climate justice pathway to 1.5 °C, Nat. Clim. Change, 8, 564–569, https://doi.org/10.1038/s41558-018-0189-7, 2018.

Roe, S.: Terrestrial Systems' Impact on and Response to Climate Change, thesis, University of Virginia, https://libraetd.lib.virginia.edu/public_view/qf85nc07m (last access: 26 August 2024), 2021.

Roe, S., Streck, C., Obersteiner, M., Frank, S., Griscom, B., Drouet, L., Fricko, O., Gusti, M., Harris, N., Hasegawa, T., Hausfather, Z., Havlík, P., House, J., Nabuurs, G. J., Popp, A., Sánchez, M. J. S., Sanderman, J., Smith, P., Stehfest, E., and Lawrence, D.: Contribution of the land sector to a 1.5 °C world, Nat. Clim. Change, 9, 817–828, https://doi.org/10.1038/s41558-019-0591-9, 2019.

Roe, S., Streck, C., Beach, R., Busch, J., Chapman, M., Daioglou, V., Deppermann, A., Doelman, J., Emmet-Booth, J., Engelmann, J., Fricko, O., Frischmann, C., Funk, J., Grassi, G., Griscom, B., Havlik, P., Hanssen, S., Humpenöder, F., Landholm, D., Lomax, G., Lehmann, J., Mesnildrey, L., Nabuurs, G. J., Popp, A., Rivard, C., Sanderman, J., Sohngen, B., Smith, P., Stehfest, E., Woolf, D., and Lawrence, D.: Land-based measures to mitigate climate change: Potential and feasibility by country, Glob. Change Biol., 27, 6025–6058, https://doi.org/10.1111/GCB.15873, 2021.

Sampaio, G., Shimizu, M. H., Guimarães-Júnior, C. A., Alexandre, F., Guatura, M., Cardoso, M., Domingues, T. F., Rammig, A., von Randow, C., Rezende, L. F. C., and Lapola, D. M.: CO_2 physiological effect can cause rainfall decrease as strong as large-scale deforestation in the Amazon, Biogeosciences, 18, 2511–2525, https://doi.org/10.5194/bg-18-2511-2021, 2021.

Seddon, N., Chausson, A., Berry, P., Girardin, C. A. J., Smith, A., and Turner, B.: Understanding the value and limits of nature-based solutions to climate change and other global challenges, Philos. T. R. Soc. B, 375, 1518–1546, https://doi.org/10.1098/rstb.2019.0120, 2020.

Seddon, N., Smith, A., Smith, P., Key, I., Chausson, A., Girardin, C., House, J., Srivastava, S., and Turner, B.: Getting the message right on nature-based solutions to climate change, Glob. Change Biol., 27, 1518–1546, https://doi.org/10.1111/gcb.15513, 2021.

Sewell, A., Van Der Esch, S., and Löwenhardt, H.: Goals and Commitments for the Restoration decade: A Global Overview of Countries' Restoration Commitments Under the Rio Conventions and Other Pledges, PBL Netherlands Environmental Assessment Agency, The Hague, 1–38, https://www.pbl.nl/en/publications/goals-and-commitments-for-the-restoration-decade (last access: 26 August 2024), 2020.

Šimpraga, M., Ghimire, R. P., Van Der Straeten, D., Blande, J. D., Kasurinen, A., Sorvari, J., Holopainen, T., Adriaenssens, S., Holopainen, J. K., and Kivimäenpää, M.: Unravelling the functions of biogenic volatiles in boreal and temperate forest ecosystems, Eur. J. For. Res., 138, 763–787, https://doi.org/10.1007/s10342-019-01213-2, 2019.

Sindelarova, K., Granier, C., Bouarar, I., Guenther, A., Tilmes, S., Stavrakou, T., Müller, J.-F., Kuhn, U., Stefani, P., and Knorr, W.: Global data set of biogenic VOC emissions calculated by the MEGAN model over the last 30 years, Atmos. Chem. Phys., 14, 9317–9341, https://doi.org/10.5194/acp-14-9317-2014, 2014.

Smith, C., Baker, J. C. A., and Spracklen, D. V.: Tropical deforestation causes large reductions in observed precipitation, Nature, 615, 270–275, https://doi.org/10.1038/s41586-022-05690-1, 2023.

Sporre, M. K., Blichner, S. M., Karset, I. H. H., Makkonen, R., and Berntsen, T. K.: BVOC–aerosol–climate feedbacks investigated using NorESM, Atmos. Chem. Phys., 19, 4763–4782, https://doi.org/10.5194/acp-19-4763-2019, 2019.

Swann, A. L. S., Fung, I. Y., and Chiang, J. C. H.: Mid-latitude afforestation shifts general circulation and tropical precipitation, P. Natl. Acad. Sci. USA, 109, 712–716, https://doi.org/10.1073/PNAS.1116706108, 2012.

Swann, A. L. S., Longo, M., Knox, R. G., Lee, E., and Moorcroft, P. R.: Future deforestation in the Amazon and consequences for South American climate, Agr. Forest Meteorol., 214–215, 12–24, https://doi.org/10.1016/J.AGRFORMET.2015.07.006, 2015.

Tai, A. P. K., Martin, M. V., and Heald, C. L.: Threat to future global food security from climate change and ozone air pollution, Nat. Clim. Change, 4, 817–821, https://doi.org/10.1038/nclimate2317, 2014.

Telteu, C.-E., Müller Schmied, H., Thiery, W., Leng, G., Burek, P., Liu, X., Boulange, J. E. S., Andersen, L. S., Grillakis, M., Gosling, S. N., Satoh, Y., Rakovec, O., Stacke, T., Chang, J., Wanders, N., Shah, H. L., Trautmann, T., Mao, G., Hanasaki, N., Koutroulis, A., Pokhrel, Y., Samaniego, L., Wada, Y., Mishra, V., Liu, J., Döll, P., Zhao, F., Gädeke, A., Rabin, S. S., and Herz, F.: Understanding each other's models: an introduction and a standard representation of 16 global water models to support intercomparison, improvement, and communication, Geosci. Model Dev., 14, 3843–3878, https://doi.org/10.5194/gmd-14-3843-2021, 2021.

U.S. Census Bureau: Percent Changes, https://www2.census.gov/programs-surveys/acs/tech_docs/accuracy/percchg.pdf (last access: 23 October 2023), 1998.

Val Martin, M., Heald, C. L., Lamarque, J.-F., Tilmes, S., Emmons, L. K., and Schichtel, B. A.: How emissions, climate, and land use change will impact mid-century air quality over the United States: a focus on effects at national parks, Atmos. Chem. Phys., 15, 2805–2823, https://doi.org/10.5194/acp-15-2805-2015, 2015.

Wang, J., Chagnon, F. J. F., Williams, E. R., Betts, A. K., Renno, N. O., Machado, L. A. T., Bisht, G., Knox, R., and Bras, R. L.: Impact of deforestation in the Amazon basin on cloud climatology, P. Natl. Acad. Sci. USA, 106, 3670–3674, https://doi.org/10.1073/PNAS.0810156106, 2009.

Weber, J., Archer-Nicholls, S., Abraham, N. L., Shin, Y. M., Griffiths, P., Grosvenor, D. P., Scott, C. E., and Archibald, A. T.: Chemistry-driven changes strongly influence climate forcing from vegetation emissions, Nat. Commun., 13, 1–12, https://doi.org/10.1038/s41467-022-34944-9, 2022.

Weber, J., King, J. A., Abraham, N. L., Grosvenor, D. P., Smith, C. J., Shin, Y. M., Lawrence, P., Roe, S., Beerling, D. J., and Martin, M. V.: Chemistry-albedo feedbacks offset up to a third of forestation's CO_2 removal benefits, Science, 383, 860–864, https://doi.org/10.1126/SCIENCE.ADG6196, 2024.

Whittaker, R. H.: Communities and Ecosystems, 2nd edn., MacMillan, New York, ISBN 0-02-427390-2, 1975.

Windisch, M. G., Davin, E. L., and Seneviratne, S. I.: Prioritizing forestation based on biogeochemical and local biogeophysical impacts, Nat. Clim. Change, 11, 867–871, https://doi.org/10.1038/s41558-021-01161-z, 2021.

Xu, R., Li, Y., Teuling, A. J., Zhao, L., Spracklen, D. V., Garcia-Carreras, L., Meier, R., Chen, L., Zheng, Y., Lin, H., and Fu, B.: Contrasting impacts of forests on cloud cover based on satellite observations, Nat. Commun., 13, 1–12, https://doi.org/10.1038/s41467-022-28161-7, 2022.

Yang, Y., Roderick, M. L., Guo, H., Miralles, D. G., Zhang, L., Fatichi, S., Luo, X., Zhang, Y., McVicar, T. R., Tu, Z., Keenan, T. F., Fisher, J. B., Gan, R., Zhang, X., Piao, S., Zhang, B., and Yang, D.: Evapotranspiration on a greening Earth, Nat. Rev. Earth Environ., 4, 626–641, https://doi.org/10.1038/s43017-023-00464-3, 2023.

Zhang, H., Li, L., Song, J., Akhter, Z. H., and Zhang, J.: Understanding aerosol–climate–ecosystem interactions and the implications for terrestrial carbon sink using the Community Earth System Model, Agr. Forest Meteorol., 340, 109625, https://doi.org/10.1016/J.AGRFORMET.2023.109625, 2023.

Zickfeld, K., MacIsaac, A. J., Canadell, J. G., Fuss, S., Jackson, R. B., Jones, C. D., Lohila, A., Matthews, H. D., Peters, G. P., Rogelj, J., and Zaehle, S.: Net-zero approaches must consider Earth system impacts to achieve climate goals, Nat. Clim. Change, 13, 1298–1305, https://doi.org/10.1038/s41558-023-01862-7, 2023.